POSTPRINT PEER-REVIEWED, ACCEPTED & PUBLISHED BY EARTH SURFACE PROCESSES AND LANDFORMS

This manuscript is a **postprint** uploaded to EarthArXiv. It has been peer-reviewed and published in *Earth Surface Processes and Landforms* on 14/07/2026, and has the DOI https://doi.org/10.1002/esp.70354. This postprint is also available via journal webpage with the "Peer-Reviewed Publication DOI" link to the right. Authors welcome comments, feedback and discussions anytime. Please, feel free to get in contact with the first author: gino.de-gelder@univ-grenoble-alpes.fr

Coral reef and mangrove interplay during Holocene sea-level changes, Belitung Island, Indonesia

T. Solihuddin[1*], G. de. Gelder[1,2*], D. A. Utami[1], F. Sidik[3], R. Rachmayani[4], M. Hendrizan[1], S. Y. Cahyarini[1], M. R. Purnama[5], D. Erkan[1], M. Widiawaty[2], M. Elliot[6], L. Husson[2]

[1]Research Center for Climate and Atmosphere, National Research and Innovation Agency, Bandung, Indonesia
[2]ISTerre, IRD, CNRS, University Grenoble Alpes, Grenoble, France
[3]Research Center for Oceanography, National Research and Innovation Agency, Jakarta, Indonesia
[4]Oceanography Research Group, Bandung Institute of Technology, Bandung, Indonesia
[5]Macrofossil Belitong, Belitung, Indonesia
[6]Laboratoire de Planétologie et Géodynamique, Université de Nantes, CNRS, France

**authors share first-authorship*

Correspondence to: Gino de Gelder (gino.de-gelder@univ-grenoble-alpes.fr)

Received: 11 September 2025 | Revised: 16 June 2026 | Accepted: 23 June 2026

DOI: 10.1002/esp.70354

RESEARCH ARTICLE

ESPL WILEY

Coral reef and mangrove interplay during Holocene sea level changes, Belitung Island, Indonesia

Tubagus Solihuddin[1] | Gino de Gelder[1,2] | Dwi Amanda Utami[1] | Frida Sidik[3] | Rima Rachmayani[4] | Marfasran Hendrizan[1] | Sri Yudawati Cahyarini[1] | Meggi Rhomadona Purnama[5] | Dilruba Erkan[1] | Millary Widiawaty[2] | Mary Elliot[6] | Laurent Husson[2]

[1]Research Center for Climate and Atmosphere, National Research and Innovation Agency, Bandung, Indonesia

[2]ISTerre, IRD, CNRS, University Grenoble Alpes, Grenoble, France

[3]Ecological Research Center, National Research and Innovation Agency, Cibinong, Indonesia

[4]Oceanography Research Group, Bandung Institute of Technology, Bandung, Indonesia

[5]Macrofossil Belitong, Belitung, Indonesia

[6]Laboratoire de Planétologie et Géodynamique, CNRS, Université de Nantes, Nantes, France

Correspondence
Gino de Gelder, Research Center for Climate and Atmosphere, National Research and Innovation Agency, Bandung, Indonesia.
Email: ginodegelder@gmail.com

Funding information
postdoctoral funding from the IRD and the Manajemen Talenta BRIN fellowship program, Grant/Award Number: 52/SIP/IV/FR/6/2022; Program PDKN Nusantara, Grant/Award Number: 083/E5/PG.02.00.PT/2022; RIIM LPDP and BRIN, Grant/Award Numbers: B-847/II.7.5/FR.00.03/2/2026, B-1158/III.4/FR00.03/2/2026; IRD postdoctoral funding to GdG; BRIN Talent Management fellowship program to GdG

Abstract

Coral reefs and mangrove forests are susceptible coastal ecosystems, particularly in light of intense human-induced pressures, including the anticipated sea level rise in the 21st century. Here, we explore the chronology and interconnectedness between coral reefs and mangroves in response to Holocene sea level changes, taking Belitung Island, Indonesia, as a case study. We described the regressive stratigraphy of an outcrop in a drained tin mine and collected a series of 3-m-long cores from three study sites, which suggests that the nearshore reef establishment was taking place at ~2-m elevation below the present mean sea level by approximately ~6.1–5.7 kyr BP. After a phase of vertical reef accretion until ca. 4.3–3.8 kyr BP, the reef system—from the forereef to onshore beaches—changed to a horizontally prograding system under conditions of relative sea level fall. The shoreline accordingly prograded seaward, leaving kilometre-wide platforms constructed by the antecedent mid-Holocene coral reefs, thereby providing accommodation space for terrestrial sediment deposition and mangrove forests that thrived from the Late Holocene onwards. The case study of Belitung Island allows us to derive general behaviour laws based on the deterministic role of geological history in the development of coastal ecosystems. By shedding light on the complex connection between coral reefs, mangroves and sea level changes over geological timescales, these results outline the need to analyse the past evolution of mangrove forests and coral reefs as a unique system to predict their future evolution.

KEYWORDS
coral reef, Holocene, Indonesia, mangrove, sea level

1 | INTRODUCTION

Coral reefs and mangrove ecosystems are key tropical ecosystems. They fringe tropical coastlines and play important ecological roles by sustaining highly diverse biological assemblages essential to coastal communities (e.g., Choudhary et al., 2024; Guannel et al., 2016). Fossil corals have been shown to document rapid changes in local ambient environmental conditions, including sea surface salinity, temperature, light, and turbidity (e.g., Cahyarini et al., 2021; Cobb et al., 2013; Falter et al., 2013; McGregor et al., 2022). In addition, fossil coral reefs document vertical land motion and sea level changes over geological timescales (e.g., Collins et al., 2011; De Gelder et al., 2022, 2023; Neumann, 1985; Solihuddin et al., 2015; Woodroffe, 2002). In this context, it is essential to understand reef evolution at geomorphological scales, as it can bridge the temporal and spatial divide between long-term geological and short-term

T. Solihuddin and G. de. Gelder share first-authorship.

ecological processes (Buddemeier & Smith, 1988; Woodroffe, 2025). Similar to coral reefs, mangrove forests provide an important habitat to a wide range of flora and fauna and function as natural carbon sequestration agents in the intertidal zones of subtropical regions (Howard et al., 2017). Mangrove environments provide fish nursery habitats, improve water quality and stabilize shorelines to support coral reefs (Rogers & Mumby, 2019; Wells & Ravilious, 2006; Whitfield, 2017). The evolution of mangroves has been closely associated with changes in sea level and climate on geological timescales, with mangroves generally flourishing during periods of relatively stable sea level (Srivastava & Prasad, 2019). Most importantly, coral reefs and mangroves develop an overlooked interconnectedness at ecological, geomorphological and geological scales. For example, coral reefs dramatically reduce the wave energy coming from offshore, allowing mangroves to grow in a calm wave environment while trapping and storing mangroves riverine sediments that might otherwise inhibit coral reef expansion (Harborne et al., 2006). Here, we contend that these interactions are not marginal but condition the development of both, making the case for mangroves and coral reefs as a unique, coupled system.

Direct observations and remote sensing provide convenient and cost-effective approaches for monitoring coastal changes (Kamila et al., 2020; Kantamaneni et al., 2022; Sui et al., 2020). However, these datasets typically span only ~30–70 years, corresponding mainly to the remote sensing era, and therefore only capture decadal-scale shoreline variability. In contrast, geological and sedimentary records document coastal evolution over millennial timescales, including responses to meter-scale Holocene relative sea level changes (Woodroffe, 2002; Woodroffe & Horton, 2005; Montaggioni, 2005). During the past ~10 000 years (the Holocene), the development of coral reefs and mangroves has been strongly influenced by relative sea level (RSL) changes, terrigenous inputs and antecedent coastal topography (e.g., Montaggioni, 2005; Woodroffe, 2025; Woodroffe et al., 2016; Yamano et al., 2019). By focusing on coastal geomorphology and stratigraphy, this study extends beyond observational records to reconstruct how meter-scale Holocene sea level variations shaped tropical coastlines. To date, relatively few studies have provided integrated stratigraphic records that simultaneously document reef development, mangrove establishment and their spatio–temporal coupling within a single coastal system. While Yamano et al. (2019) demonstrated the geomorphic control of reef flats on mangrove distribution, and Woodroffe (2025) highlighted the long-term influence of inherited coastal landforms, integrated reconstructions of their coupled Holocene evolution remain limited. Here, we provide such a reconstruction for Belitung Island.

Indonesia lies at the heart of the coral reef triangle and hosts one of the largest mangrove areas globally, much of which has experienced substantial areal decline over recent decades Global Mangrove Watch 2025). Belitung Island is located in the Karimata Strait, off the east coast of Sumatra, Indonesia, bordering the South China Sea to the north (Figure 1). It has been the focus of previous studies addressing sea level change (Meltzner et al., 2017; Suyarso, 2012), mangrove evolution (Yulianto et al., 2019) and geodynamics (Sarr et al., 2019), yet these processes have rarely been examined within a single, integrated coastal framework. This study aims to reconstruct the Holocene evolution of coupled coral reef and mangrove systems on Belitung Island to resolve the timing and mechanisms of their interaction over centennial to millennial timescales. By integrating stratigraphic, geomorphic and chronological evidence, this study demonstrates how mid-Holocene reef platforms created stable accommodation space that enabled kilometre-scale mangrove progradation during relative sea level fall, providing new insights into the long-term resilience and co-evolution of reef–mangrove systems under changing sea levels.

2 | FIELD SETTING

Belitung Island experiences a tropical climate that is strongly influenced by the seasonally reversing surface currents in the Karimata Strait and assosiated monsoonal wind systems (Xu et al., 2021). Because the regional circulation patterns are tightly coupled to the shallow bathymetry and recent evolution of the Sunda Strait, surface currents dramatically changed over the Quaternary and continuously adjust to the quickly changing bathymetry (Susilohadi et al., 2024). Currently, during the boreal winter monsoon (from November to March), southward-flowing currents from the South China Sea bring wetter conditions and lower salinity surface waters to the region. Conversely, during the boreal summer monsoon (from May to September), current directions reverse and surface waters flow predominantly westward, resulting in relatively drier conditions (Susanto et al., 2001; Wyrtki, 1961). Wave heights around Belitung Island are generally low, typically ranging between ~0.1 and 0.5 m, with higher values during the west monsoon (Pamungkas, 2018). Tides are semidiurnal, with spring tidal ranges reaching approximately 2.5–3 m (Pamungkas, 2018). Ocean temperatures in the Bangka Belitung Islands region generally range between 28°C and 30°C. The bathymetry around Belitung Island and Sunda Shelf in general is shallow, rarely exceeding depths of ~60 m (Figure 1).

Sarr et al. (2019) proposed that Belitung Island is currently subsiding at a rate of 0.2–0.3 mm/year. This subsidence is attributed to the gradual dynamic tilting of the Sunda Shelf above the subduction zone following the collision of the Australian continent with Southeast Asia (Husson et al., 2022). Because the Sunda Shelf is extremely shallow, it was a predominantly continental landmass during most of the Quaternary prior to MIS11 (around 400 kyr BP), although it was episodically inundated during the latest sea level highstands (Sarr et al., 2019). Successive marine transgressions gradually flooded the shelf, reaching Belitung only during MIS5e (around 125 kyr BP) and the Holocene. This flooding corresponds to the onset of the reef and mangrove ecosystem in the area, providing a temporal framework for analysing their long-term evolution through to modern conditions and potential future trajectories.

We focus on the northwest coast of Belitung Island (Sijuk and Batu Itam-Temparan sites; Figure 1), where the geology is dominated by the granitic Tanjung Pandan Formation, and the western coast (Petaling on Mendanau Island; Figure 1), where the basement consists of metasandstone that alternates with slate, mudstone, shale, tuffaceous siltstone and chert from the Permo-Carboniferous Kelapakampit Formation. Floodplains, river estuaries and beaches contain alluvial and beach deposits, which primarily consist of gravel, sand, silt, clay and coral fragments.

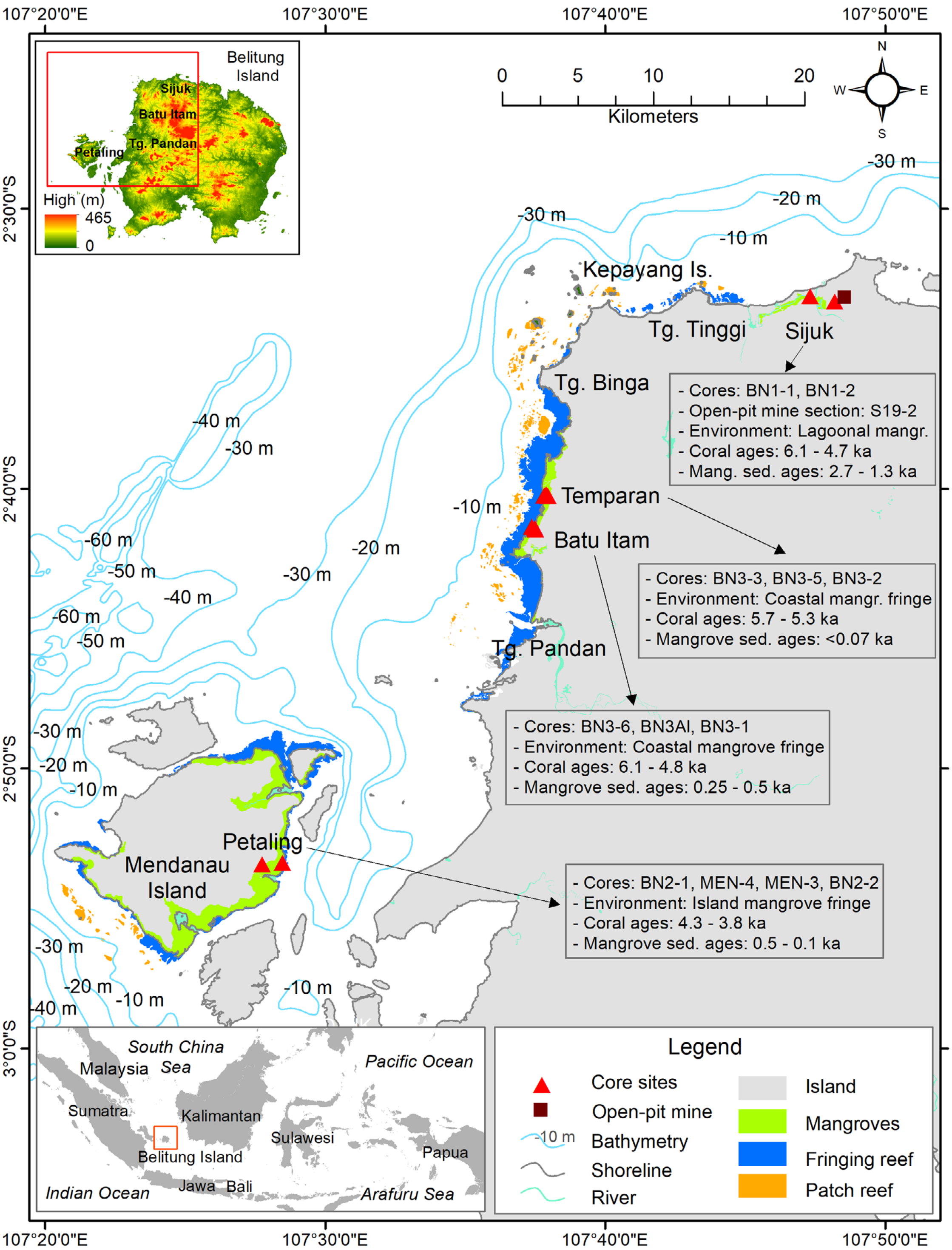

FIGURE 1 Map of study site, showing core locations (triangles), open-pit mine (rectangular) and reef-mangrove habitat distribution. Bathymetric chart from the geospatial information agency of Indonesia (BIG, 2024). Reef and mangrove habitats, as of 2021, were mapped using Sentinel-2 images, at a resolution of 10 m, and ground-truthed in 2022 and 2023.

3 | HOLOCENE SEA LEVEL RECONSTRUCTIONS AT BELITUNG ISLAND

Belitung Island is located in an area without active faults (PuSGeN, 2025) and in the far-field with respect to ice sheets, where glacio-isostatic adjustment (GIA) contributes little (< ±0.2 mm/year) to relative sea level change (Li et al., 2023; Mann et al., 2019; Tjia & Liew, 1996). Several studies constrain Holocene relative sea level variations on Belitung Island and surrounding areas (Figure 2; Geyh et al., 1979; Tjia, 1996; Hesp et al., 1998; Suyarso, 2012; Meltzner et al., 2017; Sarr et al., 2019; Yulianto et al., 2019). Early reconstructions suggested mid-Holocene sea level highstands of up to +5.8 m above present mean sea level (PMSL) in the Malacca Strait (Geyh et al., 1979), although later studies indicate more moderate regional highstands of +3–4 m PMSL (Hesp et al., 1998; Tjia, 1996). Suyarso (2012) found three separate *Ostrea* sp. fossil sites on Belitung Island. These revealed two transgressions and one regression, with sea levels 2.5 and 2.0 m above PMSL between 5 and 2.6 kyr BP, respectively. Microatoll dating

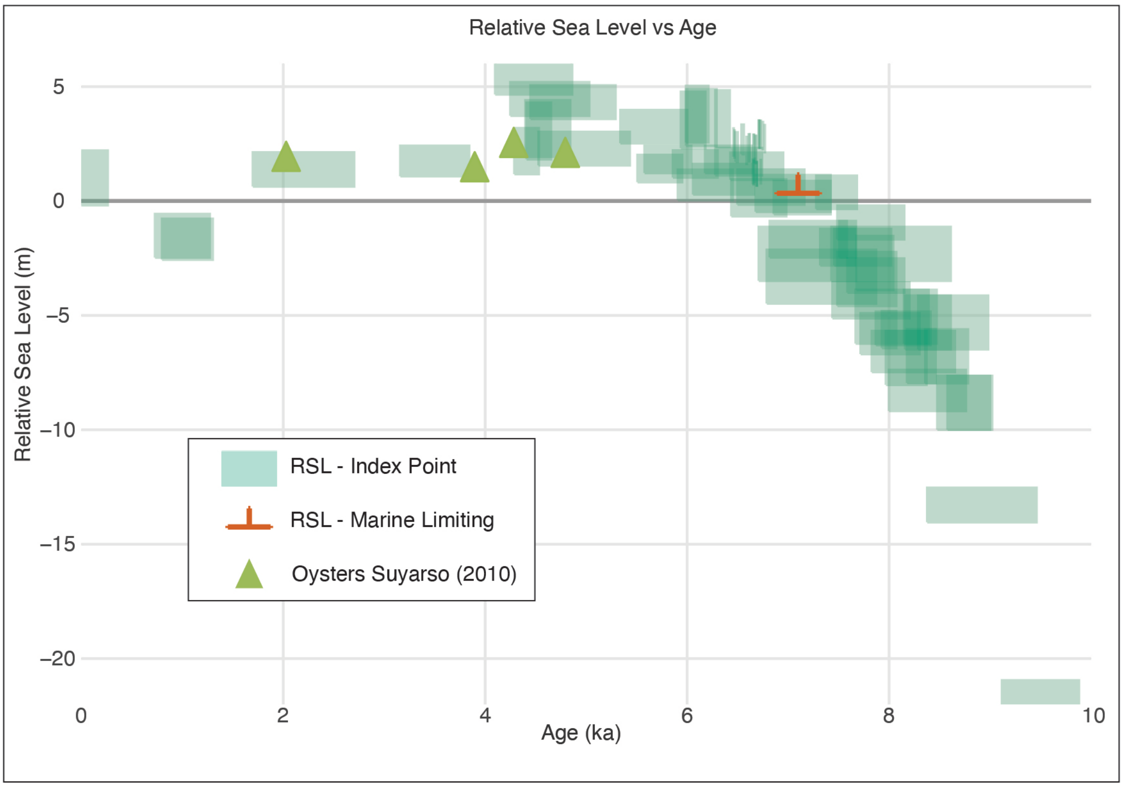

FIGURE 2 Holocene sea level reconstruction of Belitung and surrounding areas of the Sunda Shelf derived from previous studies and records, after the compilation of Mann et al. (2019), including data from Geyh et al. (1979), Tjia et al. (1983), Hesp et al. (1998), Scoffin and Tissier (1998), Kamaludin (2001), Bird et al. (2007, 2010), Scheffers et al. (2012) and Meltzner et al. (2017). We added oyster data from Suyarso (2012), but note that there are no uncertainties given. Image adapted from the HOLSEA Datahub (https://holsea-datahub-alpha.vercel.app/).

suggests a 1.5-m-high above PMSL mid-Holocene highstand at Belitung around 6.5 kyr BP (Meltzner et al., 2017). Recent regional compilations suggest that the Sunda Shelf mid-Holocene sea level peaked 0–7 m above PMSL (Li et al., 2023; Mann et al., 2019), with GIA predictions for Belitung Island around ~3 ± 3 m (Li et al., 2023).

Sarr et al. (2019) documented pronounced seaward reef progradation at Belitung Island since approximately 6.5 kyr BP, based on numerical modelling of reef growth, geomorphic observations, and radiocarbon dating of coral deposits now buried up to ~3-km inland. Similarly, Yulianto et al. (2019) found that the mangrove deposits of Belitung Island record sea level regression events dating back at least 1.5 kyr BP, implying that the coastline has prograded since then until it reached its current position. Yulianto et al. (2005) have also linked the South Kalimantan mangrove deposits to the mid-Holocene highstand, observing a transgressive phase between 9 and 5 kyr BP and a regressive sequence since then.

4 | METHODS

The distribution of reef and mangrove habitats was mapped using a Sentinel-2 image captured on 25 June 2021, with a resolution of 10 m. Habitat boundaries for reef and mangrove areas were manually digitized and saved as ArcGIS shapefiles. Overlapping between polygons was removed, and polygons were merged and corrected. The reef and mangrove distributions were ground-truthed through direct on-the-ground observations of the study area during three different field campaigns in 2022 and 2023.

A total of 10 sediment cores were collected from mangrove habitats across distinct geomorphic settings using a manual percussion corer (Solihuddin, Bufarale, et al., 2016a; Solihuddin, O'Leary, et al., 2016): two cores from the Sijuk estuary/lagoon-type mangroves, four from fringing-island mangroves at Petaling and four from exposed fringing mangroves at Batu Itam–Temparan (Figure 1). A 3-m-long, 6.35-cm-wide galvanized metal tube with a 1.6-mm wall thickness was manually hammered into the mangrove sediment. We measured compaction on-site by subtracting the length of the penetrated core from the sediment thickness after compaction, expressed as a percentage and corrected it by linearly scaling the core logs. The cores were split manually on both sides using a circular saw. The core site positions and elevations were fixed by DGPS (differential global positioning system) survey measurements. Longitude and latitude were calculated relative to the World Geodetic System 1984 (WGS 84), and elevations were plotted relative to the local mean sea level (MSL).

The terrain profile across the mangrove habitat was based on stacked swath profiles (e.g., de Gelder et al., 2022; Fernández-Blanco et al., 2019) of FABDEM (Forest and Buildings Removed Copernicus DEM) data and shallow bathymetry from the Allen Coral Atlas (2022). FABDEM is a global elevation map that removes building and tree height biases from the Copernicus GLO 30 DEM (Neal & Hawker, 2023). The data are available at 1 arcsecond grid spacing (approximately 30 m at the equator) for the globe (https://data.bris.ac.uk/data/dataset/s5hqmjcdj8yo2ibzi9b4ew3sn). The cross-section profile from FABDEM data was offset vertically to DGPS control points. The Allen Coral Atlas contains bathymetry maps at 10-m resolution, down to ~15-m depth, derived from Landsat images. They are calculated from clean coastal water mosaics, constructed over 12-month periods (Li et al., 2019).

Core logging and sampling documented characteristics include (1) sediment textural characteristics (using the Udden-Wentworth nomenclature as well as a visual assessment of sediment composition), (2) the ratio of reef framework to a matrix (after Embry & Klovan, 1971) and (3) generic coral identification (after Veron, 2000). Reef framework analysis and facies descriptions followed Montaggioni's (2005) terminology, which highlighted the growth forms of the dominant reef builders and environmental indicators.

Coral and mangrove sediments from distinct depths in each core were selected for radiocarbon dating. All coral specimens were *in situ*, based on orientation and skeletal condition and free of boring, encrustation and submarine cementation. Radiocarbon ages were obtained at the LMC14 laboratory (Saclay, France) according to their standard procedures (Dumoulin et al., 2017; Moreau et al., 2013). Radiocarbon ages were recalibrated using CALIB (http://calib.org/marine/) and the

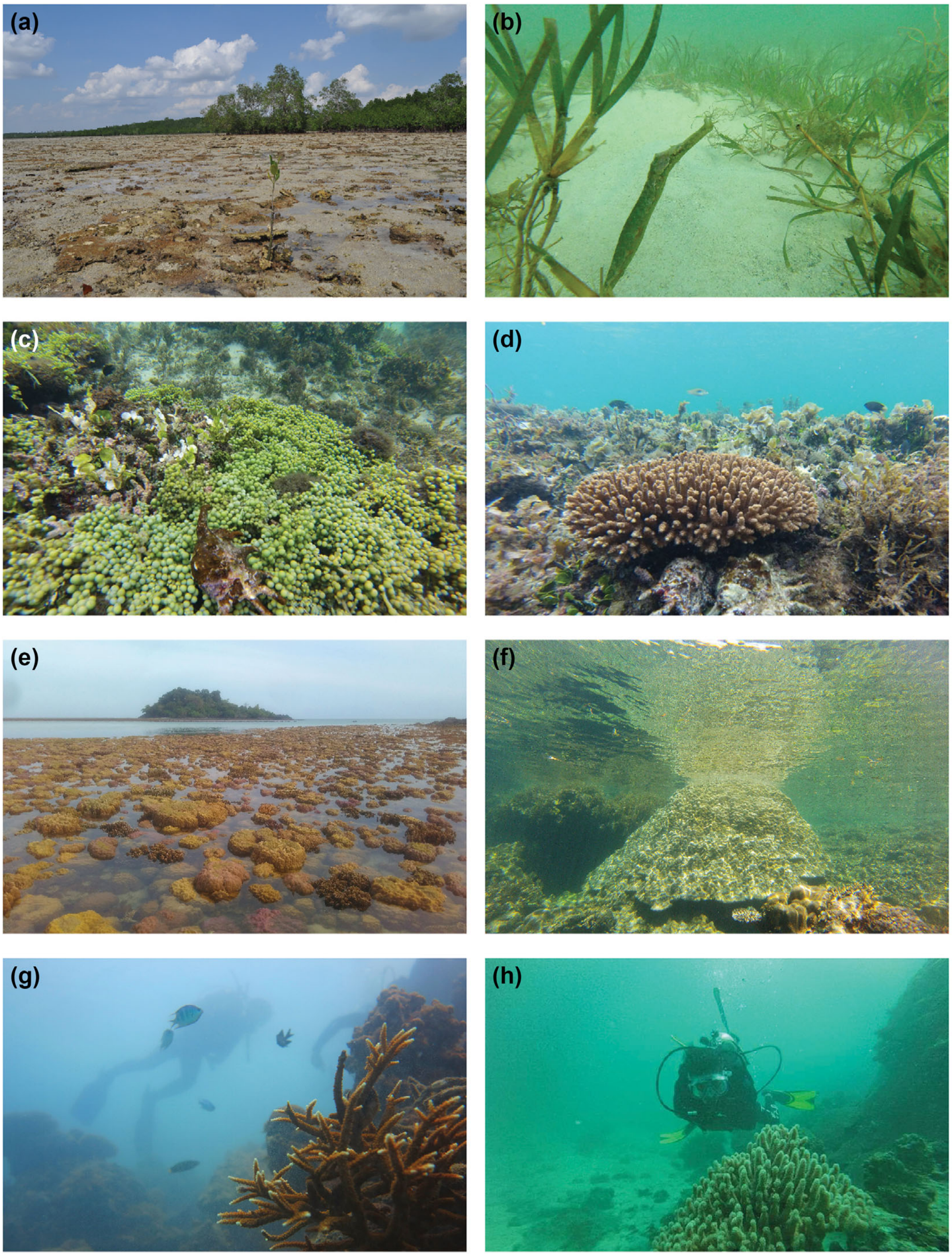

FIGURE 3 Contemporary habitats of the Belitung Island reefs, located around Batu Itam (a-d) and Kepayang Island (e-h, 107.649495°E and 2.539065°S), including (a) pioneering *Rhizophora* sp. on the intertidal reef flat, (b) seagrass on the sandy intertidal reef flat, (c) seaweeds (*Caulerpa* sp.) and spider conch (*Lambis* sp.) on the inner reef platform, (d) spider conch (*Lambis* sp.) on *Acropora* sp. corals on the inner reef platform, (e) extensive assemblages of *Porites* sp. on the outer reef platform observed during low tide, (f) domal poritids of *Porites* sp. on the outer reef platform, (g) *Acropora nobilis* on the reef foreslope associated with colonies of *Porites* sp. at depths of 3–10 m and (h) *Porites* sp. on the foreslope.

Marine20 calibration curve from Ramsey (2009) (through https://c14.arch.ox.ac.uk/oxcal/oxcal.html#). A weighted mean DR value of ±70/120 (average calculation from three nearest points) was used as the best current estimate of variance in the local open-water marine reservoir effect for Belitung Island and adjacent areas. We used the SHCal20 curve for organic materials (stems and roots) from mangrove sediments, since they do not have a reservoir correction. Ages discussed in the text are calibrated years before the present (cal year BP) with a 95.4% probability range.

5 | RESULTS

Below, we summarize the contemporary reef habitat around Belitung Island, followed by a description of the Sijuk open-pit mine, which provides a comprehensive, 3D perspective of the different facies encountered in the cores at the other sites. We then describe the geomorphology, facies and accretion history of the three study sites: Sijuk, Petaling and Batu Itam-Temparan.

5.1 | Contemporary reef habitat

The fringing reef of NW Belitung Island (Figure 1) can be categorized into four distinct eco-geomorphic zones from land to sea: intertidal beach and mangrove, inner reef platform, the outer reef platform and the fore reef slope. The intertidal beach and mangrove consist of gently sloping, medium- to coarse-sandy substrates and sometimes hard-rock Holocene reefs that support mangrove growth. On the N coast of Belitung (Figure 1; from Tg. Tinggi E-wards), mangroves typically inhabit lagoonal/estuarine environments, where they gain relative protection and receive sediment and freshwater inputs from rivers. On the sections of the N-coast characterized by rocky shores, mangroves are absent. In Petaling and Batu Itam-Temparan sections (Figure 1), mangroves grow directly on the intertidal reef flat (Figure 3a), mostly consisting of fossil corals, sand and seagrass (Figure 3b). The inner reef platform primarily consists of sand flats, mainly calcareous materials, coral rubble and encrusting coralline algae (Figure 3c,d). Living corals in this zone are sparsely distributed, primarily consisting of small colonies of *Porites* and faviids. Microatolls (up to

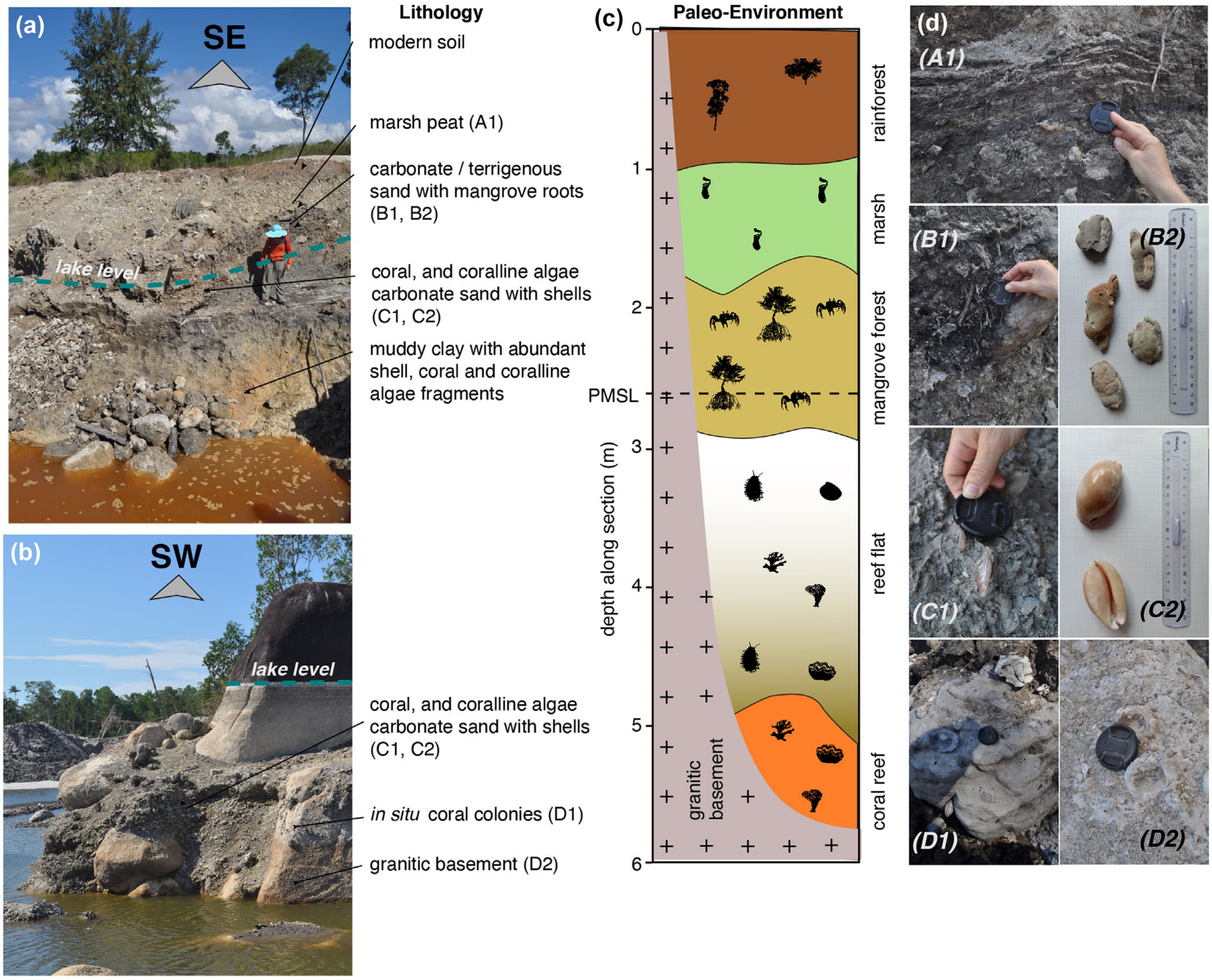

FIGURE 4 Sijuk open-pit mine outcrop (2015 – now inundated) showing the regressive sequence (coral reef, beach, mangrove forest, marsh, and rainforest). Photographs (a and b) show the lateral facies variations (water level is the common datum). Identified fossils are *Macrophthalmus latreillei* sp. (B2), *Cypraeidae fm*. (C2), *Porites* spp. (D1). The reef unit has been dated to 6310 ± 90 year BP (Sarr et al., 2019). (c) Schematic representation of interpreted paleo-environments and (d) details of the various fossils.

1.5 m in diameter) were also identified in multiple locations, predominantly *Porites* spp. The outer reef platform (Figure 3e,f) occurs seaward, where the reef flat is slightly raised. Here, living corals mainly consist of *Acropora millepora*, *Acropora hyacinthus*, *Acropora formosa*, *Acropora nobilis*, *Montipora* sp., *Pachyseries speciosa* and *Porites* sp. The forereef slope (Figure 3g,h) is characterized by a steep slope of about 30°–45° at a depth of about 10–15 m.

5.2 | Sijuk open-pit mine site

The stratigraphy of Sijuk was formerly described from observations in a drained, open-pit mine (Sarr et al., 2019), where the successive facies correspond to a regressive sequence over the granitic basement (Figure 4) that we describe here with more details. At this location [2.552075°S, 107.804542°E; S19–2 in Figure 5], an *in situ* Holocene coral reef unit is revealed by coral colonies in life position, attached to the granitic substratum (Figure 4, D2) and by large *Tridacna squamosa* and meter-scale coral colonies in pristine conditions (Figure 4, D1, *Porites* spp.). The outcrop does not expose the base of the Holocene unit, which, as a reefal system, likely lies at more than 20-m depth based on stratigraphic relationships and regional analogues (Sarr et al., 2019). A bivalve (*Tridacna squamosa*) has been dated by Sarr et al. (2019) to 6310 ± 90 year BP. This reef is overlain by laterally varying facies, whose matrix is composed of a mix of carbonate sand and muddy clay, containing abundant corals, shells and coralline algae (Figure 4, C1), some of them in pristine conditions, as, for instance, the numerous *Cypraeidae fm*. that have preserved their varnished aspect (Figure 4, C2), indicating very low transport distances.

As the sands are generally poorly sorted, we interpret this facies as reef flat deposits, ~3 m thick, with the lateral variations in the matrix reflecting local hydrodynamic conditions. This is followed by an ~1-m-thick sandy facies, rich in roots and crabs (*Macrophthalmus latreillei* sp., Figure 4, B2; although most fossils were found at another mine site 800 m to the SW), characteristic of a mangrove environment. A ~1-m-thick peat unit follows, which we interpret as a possibly brackish marsh. A soil unit of variable thickness caps the sequence, covered by the Belitung rainforest.

5.3 | Sijuk site

The area of Sijuk is geomorphologically characterized by dissected hills, with the highest point reaching 60 m above sea level (Figure 1). The coast of Sijuk is characterized by sandy beaches fronting a low-lying coastal plain with low-relief dune morphology (Figure 5), overlain by shrubs and coastal vegetation. Mangroves in Sijuk grow in sheltered locations, particularly in lagoon areas and rivers (Figures 1 and 5), where there is a vast, fluvial-dominated environment, according to the mangrove environmental setting from Woodroffe (1992). *Rhizophora* and *Bruguiera* are the main types of mangroves in the area. They grow on a substrate of unconsolidated, brownish to blackish sand mixed with coarse to very coarse quartzite sand. There are no fringing reefs along the sandy coastlines, but there are offshore patch reefs with irregular margins and unbroken margins, measuring lengths and widths of less than 500 m and 300 m, respectively (Figures 1 and 5). The distribution of both mangroves and coral reefs is affected by irregular topographic and bathymetric peaks of granitic basement rock that crop out onshore and offshore (Figure 5).

Two cores (BN1-1 and BN1-2) were collected in the mangrove habitat approximately 2.5 and 1 km from the coastline, respectively (Figure 5). The elevations of the two core positions are 0.94 and 0.76 m above PMSL, respectively. Both BN1-1 and BN1-2 have a maximum depth of 2.8 m of core penetration and 32% compaction during coring. However, Holocene sedimentary facies are significantly different between the two cores. The top ~1.25 m of BN1-1 is composed of brownish organic sand with abundant mangrove roots mixed with coarse to very coarse quartzite sand. At depths between 1.25 and 2.8 m below ground level, there are coral fragments consisting mainly of branching corals (both robust and arborescent), as well as various other genera of domal and foliaceous corals (Figure 5). Acroporids are the most common branching corals encountered on the core, but fragments of domal coral from *Porites* sp. are also common, as is foliaceous coral from the genus *Montipora*. Muddy clay and a medium-sand matrix dominate the sediments throughout the reef section, transitioning into organic sand at the top layer. The top ~1.33 m of core BN1–2 consists of loose, coarse, brown quartzite sand mixed with organic sand with abundant mangrove roots and trunks. The rest of the core, from ~1.33 to 2.8 m deep, is made up of brown organic sand mixed with poorly sorted, medium- to coarse-sand (Figure 5).

Five radiometric ages from corals and mangrove sediments were collected from two cores at Sijuk (Table 1). The oldest age, 6.1–5.6 kyr BP, was obtained from a coral fragment at the base of core BN1-1, about −1.83 m below present MSL. The younger age, 5.2–4.7 kyr BP, was obtained on a coral fragment from the midpoint of core BN1-1 around −0.55 m below present MSL, which yields a mean accretion rate of 1.42 ± 0.56 mm/year if we use ±0.05 m as depth uncertainty. The base of mangrove sediments within BN1-1 at −0.24 m below the present MSL has a radiometric age of <65 years BP, which we attribute to young root contamination. In contrast, the ages from the BN1-2 core are much younger than the coral ages at BN1-1, showing 2.7–2.3 and 1.7–1.3 kyr BP at −1.54 and −0.54 m below PMSL, respectively. This value indicates an accretion rate of 0.90 ± 0.21 mm/year between the two samples and a rate of 1.00 ± 0.11 mm/year between the upper sample and the top of the core.

5.4 | Petaling site

Petaling is located on Mendanau Island, west of Belitung Island, and is geomorphologically characterized by highly dissected hills, with the highest point reaching 80 m above MSL (Figure 1). The coast of Petaling is predominantly characterized by mangrove habitat, with narrow fringing reefs and scattered patch reefs offshore (see Figures 1 and 6). Mangroves at Petaling form dense stands along the coast, supported by a broad (up to 0.5 km) low-gradient intertidal zone suitable for mangrove colonization (Woodroffe, 1992). *Rhizophora* and *Avicennia* are the dominant mangroves in the area, which sit on unconsolidated, dark brownish organic sediments intercalated with poorly sorted, medium- to coarse-sand. The reef flat is mostly occupied by sand sheets and coral rubble. Irregular topographic features consisting of meta-sandstone basement rocks crop out onshore (Figure 6), affecting the distribution of mangroves. The patch reefs

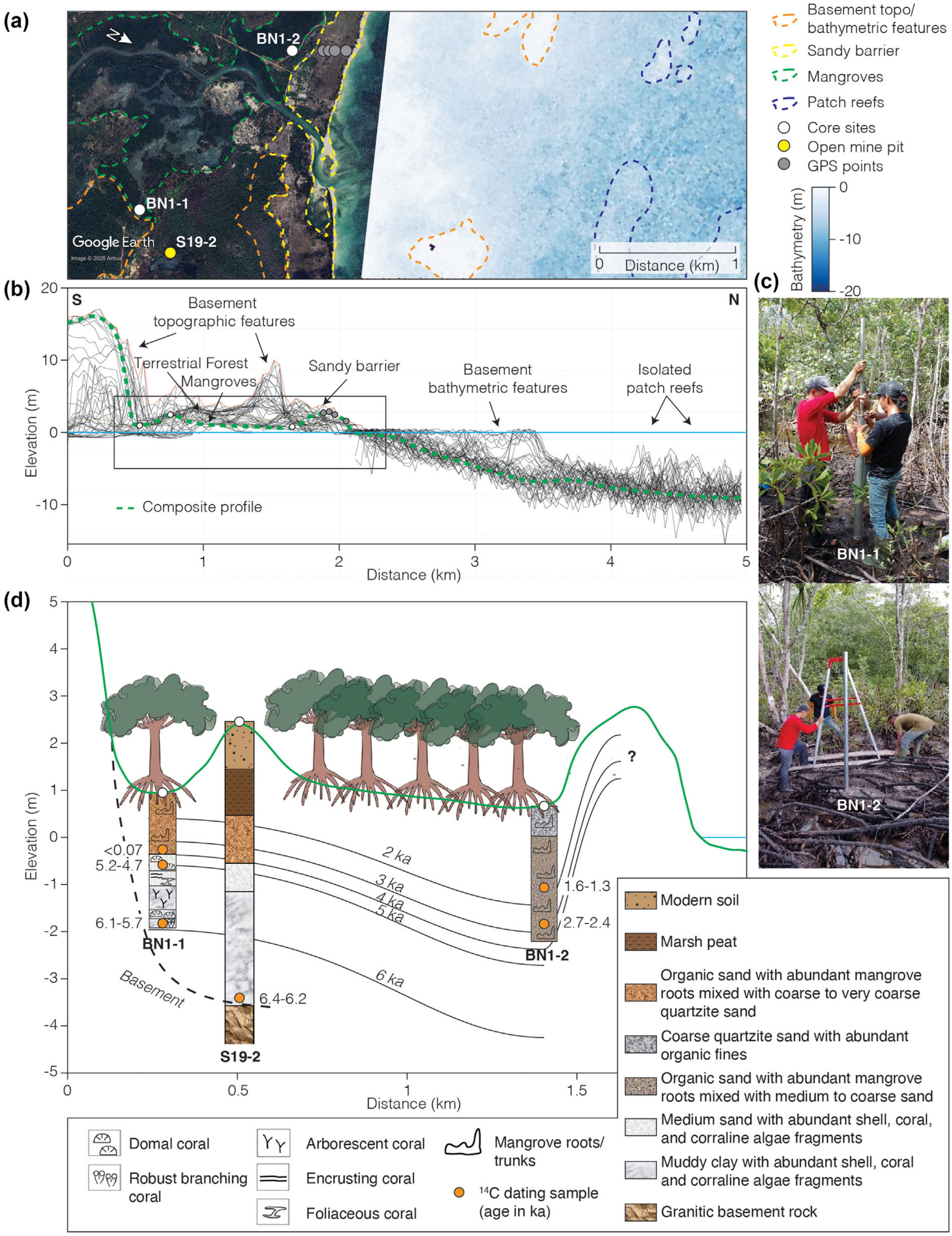

FIGURE 5 Cross-section of the Sijuk core locations and open-pit mine (S19–2) with (a) a map combining Landsat imagery and Allen Coral Atlas bathymetry. (b) Stacked swath profile across the map with coast-perpendicular profiles every 30 m. The composite profile combines GPS measurements with representative sections of the morphology used in panel d. (c) Field photographs of the core sites and (d) isochrons based on radiocarbon dating results and a summary of the core logs that display Holocene sedimentary facies as well as the open-pit mine at ~2.5 m above PMSL.

offshore seem to occur along a bathymetric high that is the continuation of an island to the NNE (Figure 1).

Four cores (BN2-1, MEN-4, MEN-3 and BN2-2) were taken in the mangrove habitat approximately 0.1, 0.5, 1.0 and 1.5 km from the coastline, respectively (Figure 6). The maximum depths of BN2-1, MEN-4, MEN-3 and BN2-2 core penetration are 2.7, 1.5, 1.7 and 1.5 m, and compaction during coring was 37%, 34%, 32% and 20%, respectively. The Holocene sedimentary facies of BN2-1, BN2-2 and

TABLE 1 Radiocarbon dates from coral and organic materials from mangrove sediments across study sites.

Site	Sample code	Lab code	Material	Elevation relative to PMSL (m)	Delta C13	Conventional age (BP)	Calibrated age (cal year BP)
Sijuk	BN1-1 (24–29)	SacA68616	Mangrove sediments	0.38	−30.7	After 1950	<70
	BN1-1 (55–58)	SacA68606	Coral	0.12	−3.2	4805 ± 30	5245–4724
	BN1-1 (183–185)	SacA68607	Coral	−1.76	−4.3	5630 ± 30	6118–5665
	BN1-2 (87–91)	SacA68617	Mangrove sediments	−0.55	−35.7	1525 ± 30	1587–1302
	BN1-2 (155–160)	SacA68618	Mangrove sediments	−1.55	−34.2	2495 ± 30	2754–2364
Petaling	BN2-1 (55–59)	SacA68619	Mangrove sediments	−1.44	−28.3	215 ± 30	471–132
	BN2-1 (82–86)	SacA68620	Mangrove sediments	−1.96	−30.0	After 1950	<70
	BN2-2 (40–44)	SacA68621	Mangrove sediments	0.51	−28.2	After 1950	<70
	BN2-2 (66–69)	SacA68622	Mangrove sediments	0.25	−27.2	After 1950	<70
	MEN-3 (OSL base)	SacA70699	Coral	−0.75	−4.5	4120 ± 30	4337–3826
Batu Itam-Temparan	BN3-1 (75–82)	SacA68624	Mangrove sediments	−0.3	−26.6	215 ± 30	251–504
	BN3-2 (58–61)	SacA68625	Mangrove sediments	0.1	−30.6	After 1950	<70
	BN3-AI (20)	SacA68604	Coral	0.0	1.1	4790 ± 30	5238–4711
	BN3-AI (80)	SacA68605	Coral	−0.68	−1.4	4870 ± 30	5289–4822
	BN3-5 (4–11)	SacA68608	Coral	0.72	−6.7	5225 ± 30	5676–5257
	BN3-5 (29–33)	SacA68609	Coral	0.32	−1.7	5295 ± 30	5742–5308
	BN3-6 (8–10)	SacA68610	Coral	−0.07	−6.8	4830 ± 30	5270–4786
	BN3-6 (75–78)	SacA68611	Coral	−0.97	−2.4	5590 ± 30	6094–5621

Note: Calibrated age represents a 95.4% confidence interval. All samples were dated at Laboratoire de Mesure du Carbone 14 (LMC14; Saclay, France).

MEN-4 are very similar. They have a top layer of loose, dark brownish organic sand with many mangrove roots and trunks mixed in with poorly sorted, medium- to coarse-sand and a bottom layer of meta-sandstone rock. For BN2-1, MEN-4 and BN2-2, the lithological contact between unconsolidated organic sand and basement rock is 1.85, 1.46 and 1.09 m deep below ground, respectively. The top section of MEN-3 consists of sand alternating with layers rich in dark brown organic material, while a coral layer lies beneath it at a depth of 85 cm below ground (Figure 6).

Five radiometric dating samples were obtained from one coral sample and four dark brown bulk sediment layers, collected from three cores at Petaling (Table 1). Out of the four sediment samples, three were younger than 70 years BP and probably erroneous due to young root contamination, indicating that these samples may not accurately reflect the true age of the sediment layers. The radiocarbon date from BN2-1, obtained from a bulk sediment layer taken at −1.69 m below PMSL, shows an age of 471–132 years BP, and MEN-3, taken at −1.73 m below PMSL, reveals an age of 4.3–3.8 kyr BP.

5.5 | Batu Itam-Temparan sites

Batu Itam-Temparan is located on the NW coast of Belitung Island and is geomorphologically characterized by highly dissected undulating plains of denudational origin, with the highest point reaching 40 m above PMSL (Figure 1). The coasts of Batu Itam-Temparan are predominantly characterized by mangrove habitat along the shore with an extensive intertidal fringing reef and scattered patch reefs offshore (see Figures 1 and 7). *Rhizophora* and *Avicennia* are the dominant

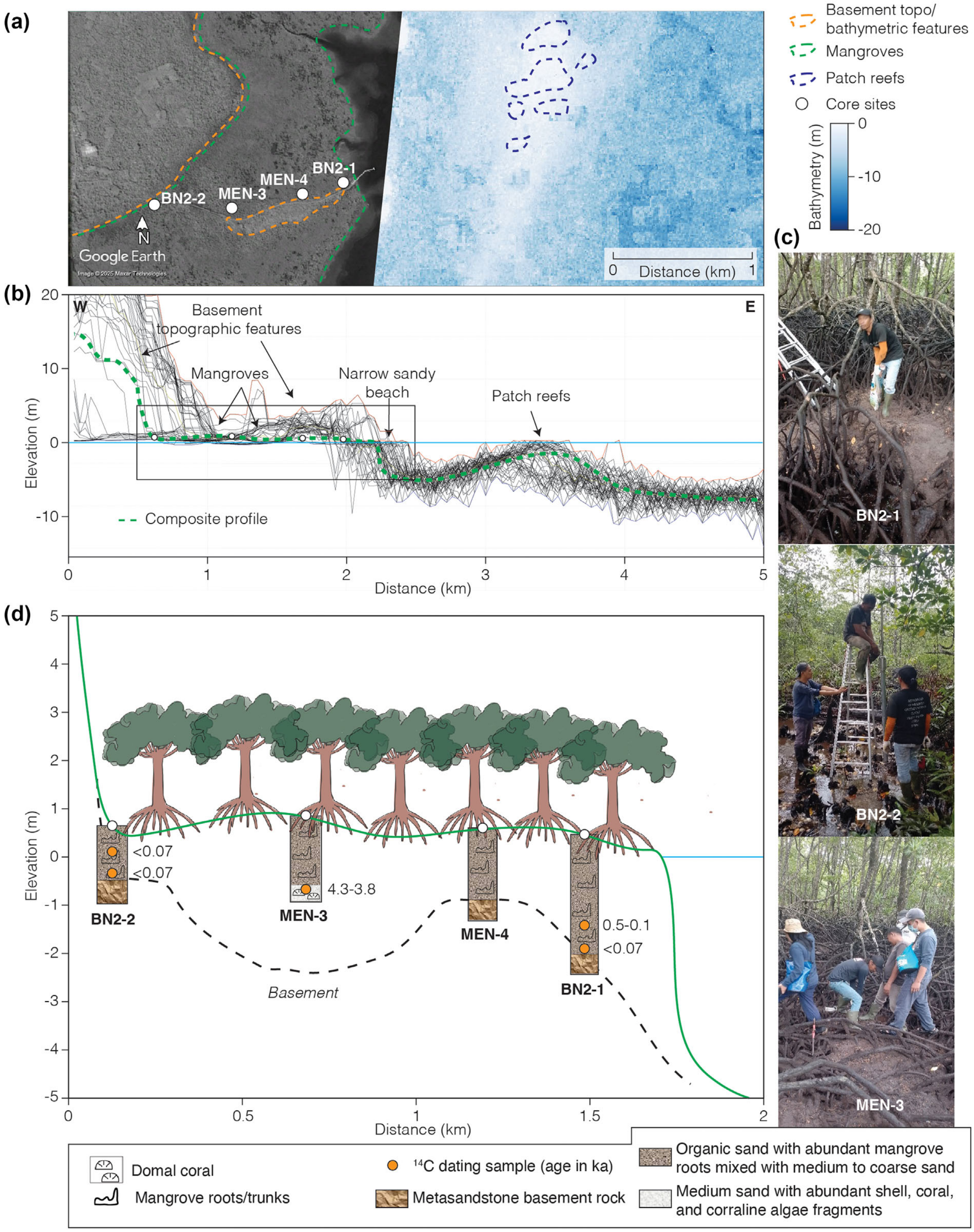

FIGURE 6 Cross-section of the Petaling core locations with (a) a map combining Landsat imagery and Allen coral atlas bathymetry. (b) Stacked swath profile across the map with coast-perpendicular profiles every 30 m. The composite profile combines GPS measurements with representative sections of the morphology used in panel d. (c) Field photographs of the core sites and (d) a summary of the core logs that display Holocene sedimentary facies.

mangroves in the area, sitting on unconsolidated brownish to blackish organic layers alternating with sand. The reef flat, which stretches approximately 2.3 km seaward, is composed of carbonate sand, coral rubble, encrusting coralline algae, encrusting corals, microatolls (up to 1.5 m in diameter), sparse small living coral colonization and predominantly *Thalassia* seagrass with a height of 10–15 cm. The reef crest forms a low, slightly emergent ridge at the reef edge.

Six cores (BN3-1, BN3-2, BN3-3, BN3-5, BN3-6 and BN3-Al) were taken on the mangrove habitat at two different coast sections, including three cores (BN3-1, BN3-6 and BN3-Al) at Batu Itam and

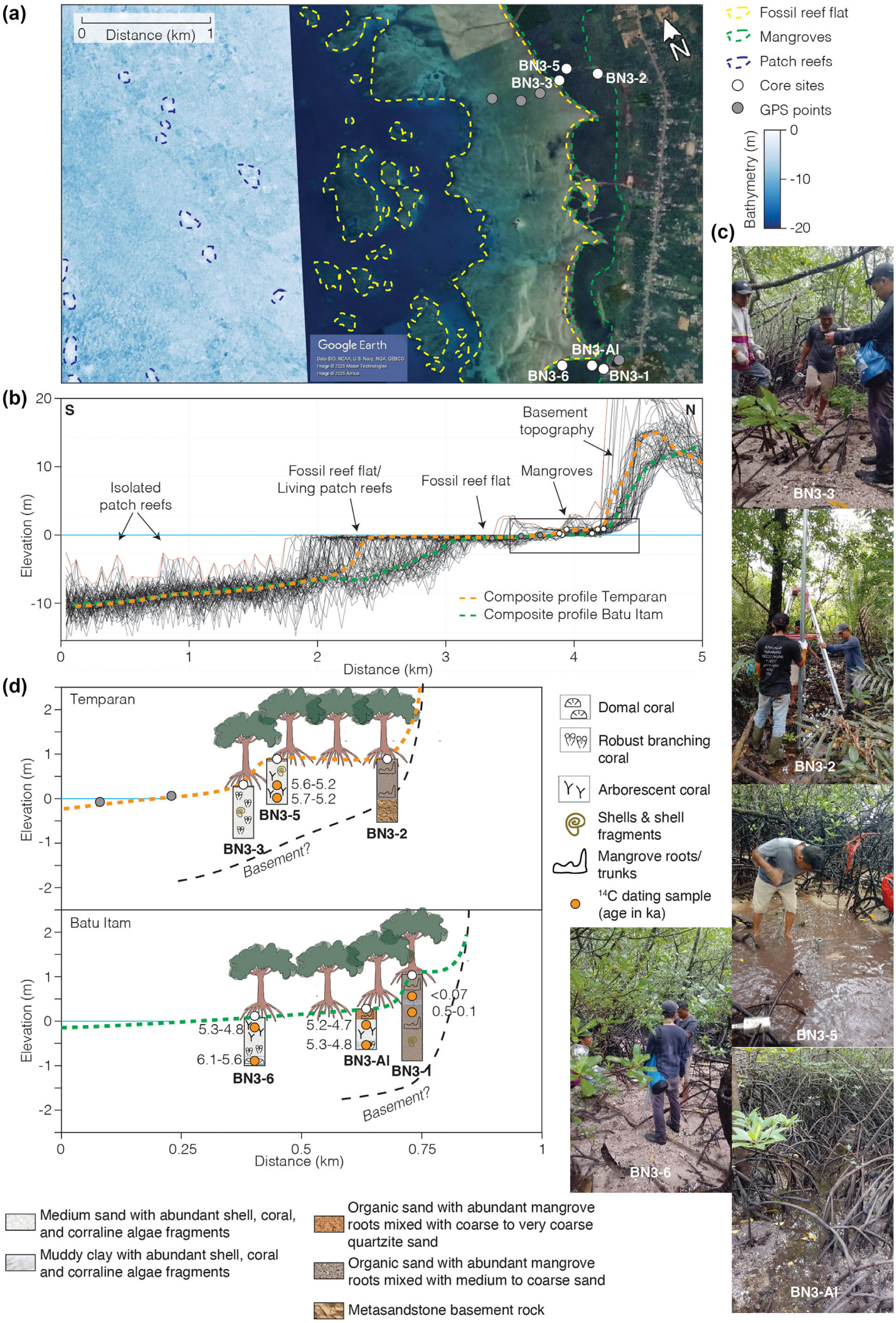

FIGURE 7 Cross-section of the Temparan and Batu Itam core locations with (a) a map combining Landsat imagery and Allen Coral Atlas bathymetry. (b) Stacked swath profile across the map with coast-perpendicular profiles every 30 m. The composite profile combines GPS measurements with representative sections of the morphology used in panel d. (c) Field photographs of the core sites and (d) a summary of the core logs that display Holocene sedimentary facies.

three cores (BN3-2, BN3-3 and BN3-5) at Temparan (Figure 7). The maximum depths of BN3-1, BN3-2, BN3-3, BN3-5, BN3-6 and BN3-Al core penetration are 2.8, 1.3, 1.6, 1.1, 1.0 and 0.8 m, and compaction during coring was 35%, 19%, 49%, 41%, 24% and 13%, respectively. The Holocene sedimentary facies of BN3-3, BN3-5, BN3-6 and BN3-Al are quite similar. They consist of a thin layer of loose, brownish-to-blackish organic sand with many mangrove roots at the top 0.2 m. Below the sand with abundant organic fines is coral reef facies, comprising arborescent, robust branching and dome-shaped corals with an unconsolidated, brownish grey, sandy matrix. The branching coral clasts on BN3-3, BN3-5, BN3-6 and BN3-Al are mostly made up of arborescent and robust acroporids. However, the bottom section of the BN3-6 core also contains domal coral from the genus *Porites* sp. (Figure 7). BN3-1 and BN3-2 are exceptions. BN3-1 consists of unconsolidated dark grey, very fine- to fine-grained sand with shell fragments, gastropods, molluscs, rock fragments and roots at the base; a thin layer of unconsolidated coarse quartzite sand mixed with blackish organic sediment; and a top layer of unconsolidated dark brownish organic sediment mixed with fine- to coarse-grained quartzite sand. BN3-2 consists of organic sand at the top and basement rock at the bottom (Figure 7).

Six radiometric ages were obtained from corals collected from Batu Itam (Table 1). The base of BN3-6 yielded the oldest age, 5.9–5.4 kyr BP, approximately −0.97 m below present MSL. The base of core BN3-5 (−0.1 m below present MSL) and BN3-Al (−0.56 m below present MSL) recorded relatively similar ages of 5.5–5.1 and 5.1–4.5 kyr BP, respectively. The upper layer of the BN3-Al core is the youngest age, 5.0–4.5 kyr BP, approximately −0.1 m below present MSL. The upper layers of BN3-6 (−0.3 m below present MSL) and BN3-5 (+0.15 m above present MSL) recorded a relatively similar age of 5.0–4.5 and 5.5–5.0 kyr BP, respectively. Thus, the accretion rates of BN3-Al, BN3-6 and BN3-5 were 5.7 ± 25, 0.8 ± 0.4 and 4.3 ± 22 mm/year, respectively. One radiometric age from mangrove sediments collected at Batu Itam (BN3–2) was younger than 70 years BP and is likely erroneous due to young root contamination (Table 1). The other one at BN3-1 was also young but possibly more reliable, with a calibrated age of 251–504 year BP (Table 1).

6 | DISCUSSION

6.1 | Sedimentary facies and accretion

We identified two distinct facies based on their constituent materials: coral and mangrove facies. Coral facies are situated directly below the mangrove facies, with no terrigenous sediment layer in between. In terms of paleo-environments described in Figure 4, they would correspond to a reef-flat environment. Mangrove facies (corresponding to a mangrove forest in Figure 4) are situated either on top of coral facies or directly on top of basement rock types (granites or meta-sandstone).

The coral facies are characterized by the presence of carbonated skeletons and grains that originate from the coral reef environment. The composition comprises four primary subfacies: domal, robust, arborescent and folliaceous. Most of the coral fragments are fresh and seem to be in their original position, with poorly sorted sediments intercalated with the reef fragments, which is indicative of a reef flat environment. The ages of these coral facies range from ~6 kyr BP (BN1-1, BN3-6) to ~4 kyr BP (MEN-3), but older bivalve samples have been reported by Sarr et al. (2019; 7.3–6.3 kyr BP) at the Sijuk open mine-pit site. The matrix sediment composition varies between Sijuk and Batu Itam–Temparan. At Sijuk, the matrix sediments are almost evenly split between poorly sorted medium-sand and muddy clay (see Figure 5). At Batu Itam–Temparan, however, the matrix sediments are primarily composed of poorly sorted medium sand. This suggests that they had distinct depositional environments during the Holocene, indicating that Sijuk had a more sheltered reef environment and is possibly more influenced by fluvial runoff events compared to Batu Itam–Temparan.

- Domal coral subfacies are dominated by dome-shaped poritids (mostly *Porites* sp.). On Belitung Island, domal coral subfacies in a sandy matrix are more prevalent at Sijuk. As postulated (Cabioch et al., 1999; Done, 1982; Grossman & Fletcher, 2004; Hibbert et al., 2016; Montaggioni, 2005), domal coral colonies tend to occupy lower energy reef settings, from the surface to depths of around 10–15 m. Here, the subfacies inhabit a nearshore environment and relict reef flats and are located relatively in the upper part of the reef section.
- Robust-branching coral subfacies are dominated by acroporids from the genus *Acropora formosa* associated with domal poritids (*Porites* sp.). On Belitung Island, the distribution of robust-branching coral colonies in a sandy matrix is more common at Batu Itam-Temparan. They are located in a relatively shallow paleoenvironment, with water depths of less than ~2 m in most of the sampled cores. Similar to this, Montaggioni's (2005) description of the Indo-Pacific robust-branching coral facies suggests that this facies is widely distributed on the outer reef flat to the upper forereef zones.
- Various thin-branched corals dominated by acroporids form arborescent-branching coral subfacies on Belitung Island. The cores of both Sijuk and Batu Itam-Temparan contain these subfacies. At Sijuk, this facies disperses in a muddy clay matrix in relatively deeper water (~2–2.5 m), while at Batu Itam-Temparan, it disperses in a medium sand matrix at a depth of less than 1 m. The type of coral resembles Montaggioni's (2005) description of arborescent coral, which usually grows on shallow inner reef flats and back reef slope zones (Hopley et al., 2007).
- Foliaceous coral subfacies is encountered on the upper part of the Sijuk core at a depth of approximately 1.5–2 m below ground (see Figure 5). The coral clasts primarily consist of platy *Montipora* sp. colonies embedded in an unconsolidated dark grey medium sand matrix, which also includes coral debris, gastropods, bivalves and foraminifera tests. Montaggioni (2005) found similar patterns in the Holocene reef sections of the Indo-Pacific regions. These patterns show that the foliaceous coral facies grows in protected reef environments that usually have a lot of suspended sediment (Kleypas, 1996; Montaggioni & Faure, 1997; Takahashi, 1988). This facies is frequently colonized by arborescent coral communities in water depths of less than 15 m (Done, 1982; van Woesik & Done, 1997; Yamano et al., 2001).

The mangrove facies is distributed either above the coral facies or basement rock, with a thickness of up to 2.5 m. It can be found in

Sijuk, Petaling and Batu Itam-Temparan, but the ratios between mangrove organic matter and sands are markedly different in each location. It is made up of loose, brownish to blackish sand with abundant mangrove roots in it. Mangrove progradation likely reflects a combination of low hydrodynamic energy and geomorphic controls exerted by the underlying reef-flat morphology. Wide and gently sloping reef flats are known to dissipate wave energy efficiently and promote sediment retention, thereby facilitating mangrove establishment and seaward expansion (Kench & Brander, 2006; Woodroffe, 2002). Although wave conditions across all sites are generally low with nearshore wave heights rarely exceeding 0.8 m, modest variations in far-field wave energy appear between sites. We extracted wave energy data from the Changing Shores Google Earth Engine application (Nienhuis et al., 2020), indicating the lowest wave energy at Petaling (~0.4 J/m^2), slightly higher at Batu Itam-Temparan (~1.7 J/m^2), and the highest estimate at Sijuk (~2.8 J/m^2). We suggest this may contribute to the observed variability in mangrove extent, with more extensive mangrove progradation occurring under lower energy conditions (Alongi, 2008; Mazda et al., 1997) for the fringing mangroves. In addition, the higher wave energy at Sijuk promoted the establishment of extensive sandy barriers, which are currently overlain by dunes (see Figure 5), creating a relatively calm environment conducive to the development of lagoonal reefs, tidal creeks and mangroves. The ages derived from mangrove sediments span from the late Holocene (2.7–2.3 kyr BP) to the near past (471–132 years BP) (Table 1). The modern mangrove types are dominated by *Rhizophora*, *Bruguiera* and *Avicennia*, sitting on the relict reef flat and/or basement rock.

Apparent accretionary rates appear similar for coral reef system deposits compared to mangrove deposits (Figure 8), although we have only one site with multiple reliable mangrove deposit ages. And although the position and preservation of coral samples suggest they are found *in situ*, we cannot be completely sure that the ages of the coral samples are the same as the ages of deposition, as coral fragments may travel short distances on the reef flat. Taking the ages at face value, apparent accretion rates for coral fragments range from 0.8 ± 0.4 to 5.7 ± 25 mm/year. The corals at the higher elevation, between ~0.6 m below MSL and ~0.7 m above MSL, from Batu Itam (BN3-AI) and Temparan (BN3-5), showed the fastest accretion rates (Figure 7), but given that the coral ages that determine the rates are very similar, the resulting high error margins make it difficult to interpret these rates. The mangrove accretion rate for BN1–2 is 0.9 ± 0.2 mm/year between ~2.5 and ~1.5 kyr BP and a very similar 1.0 ± 0.1 mm/year between ~1.5 kyr BP and the present (top of the core). The younger samples, from BN2-1 and BN3-1, indicate much higher rates of 6.3 ± 3.6 and 3.2 ± 1.1 mm/year, respectively. Larger compilations also reveal similar discrepancies. Modern fringe-type mangrove forests show ranges from a low of 1.6 to a high of 8.6 mm/year (Woodroffe et al., 2016), a range that our rates for BN2-1 and BN3-1 fall well within. A global compilation of 78 Holocene mangrove sequences showed ranges of ~0.2–2.0 mm/year vertical accretion rates for the past 6 kyr BP (Saintilan et al., 2020), a range that our accretion rates for BN1-2 fall well within. One reason for these discrepancies could be that mangroves are very dynamic in terms of sedimentary settings, where periods of rapid deposition may alternate with periods

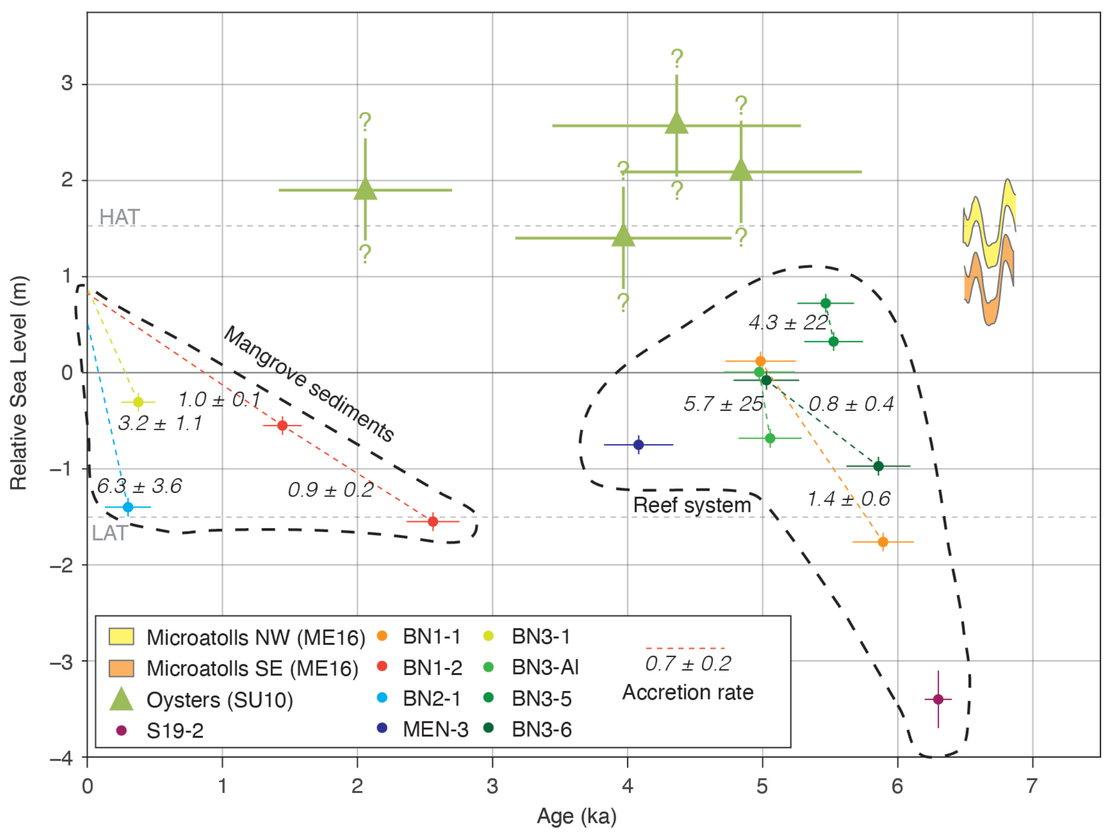

FIGURE 8 Dated core samples with their elevation relative to PMSL and apparent accretion rates, compared to relative sea level estimates for Belitung Island derived from microatolls (Meltzner et al., 2017) and oysters (Suyarso, 2012, vertical uncertainty not mentioned). HAT = highest astronomical tide and LAT = lowest astronomical tide are represented with grey dashed lines. Accretion rates for mangrove samples (BN1-2, BN2-1, BN3-1) are calculated assuming the ages of the core tops were 0 year.

of erosion (e.g., Nathan et al., 2025), and the short-term rates over a few hundred years are not necessarily representative of Holocene rates. Another reason might be that BN2-1 and BN3-1 mangrove sediment samples have been contaminated as well by younger roots, as for several of the samples dated <70 years (Table 1).

6.2 | Chronology of Holocene coral reef and mangrove interplay

On Belitung Island, we divide the chronology of the Holocene coral reef system (including the reef and onshore beach deposits) and mangrove buildup into two phases: nearshore reef establishment and mangrove development show that these two regimes closely reflect RSL variations.

Coring limits precluded Pleistocene reefs, which are presumed to be present below 20–30 m below PMSL around Belitung Island (Sarr et al., 2019). Similarly, we can infer that Holocene reef units, older than the 6.5 kyr BP sample at S19-2, exist at lower elevations and further seawards above the Quaternary reef unit (Figure 9). However, given the lack of chronological constraints prior to ~6.5 kyr BP, we limit the following discussion to the mid- to late-Holocene period.

The Holocene sea level curve for the Sunda Shelf (Figure 2) indicates that the reef near the Sijuk open-pit mine established shortly after rising sea levels inundated the antecedent substrates, around 6.5 kyr BP (Figure 8). RSL estimates for Belitung from microatoll data (Meltzner et al., 2017) are 4–6 m above the coral sample of S19-2 of comparable age (Figure 8), suggesting that the sampled reef in Sijuk was growing at several meters below sea level around 6.5 kyr BP. Both regional paleo-sea level indicators (Figure 2) and the Belitung oyster fossils of Suyarso (2012); Figure 8) suggest that elevated mid-Holocene sea level (>2 m above PMSL) persisted until around ~4.5 kyr BP. Although Suyarso (2012) did not provide vertical measurement uncertainties or indicative ranges, modern ecological studies show that intertidal oysters commonly occupy a vertical zone spanning from approximately MSL to the upper intertidal zone (e.g., Hopley et al., 2007). However, we acknowledge that such ecological ranges may vary between regions depending on tidal regime and hydrodynamic conditions. Field observations in Belitung indicate that living oysters are typically found within approximately ~30 cm of PMSL, which provides a local observational constraint but should be regarded as an approximate indicative range rather than a calibrated vertical uncertainty. Based on these combined constraints, we infer that the ~4–6 kyr BP corals dated in this study, deposited between ~0.8 m above and ~1.7 m below PMSL, most likely formed in a reef flat (Petaling and Batu Itam-Temparan) or shallow lagoon (Sijuk).

In general, during the period of ~6.5 to ~4 kyr BP, the reef around Belitung was aggrading, with (1) a consistent age-depth decrease in Sijuk for S19-2 and core BN1-1, from ~6.3 kyr BP at ~3.5 m below PMSL (S19–2) to ~5 kyr BP at ~0.5 m below PMSL (Figure 4); (2) reef infill occurred between the basement topography in Petaling until ~4 kyr BP (Figure 6); and (3) similar ages of ~5 kyr BP were found at ~0.2 m below PMSL between BN3-Al and BN3-6 over a distance of a few hundred meters in Batu Itam (Figure 7). On top of aggradation, some progradation also has occurred, especially in Sijuk, where a former lagoon was progressively filled with reef and mangrove sediments (Figure 5). Other than attesting to sedimentary progradation, the depth of the ~2.5 kyr BP mangrove sediments at ~1.5 m below PMSL also implies that RSL must have been close to present-day elevations by that time, given the ±1.5 m intertidal range providing mangrove habitat (Figure 8). This also implies the ~2 ka oyster sample at ~2 m above PMSL (Figure 8; Suyarso, 2012) lived close to HAT. The sandy barrier in Sijuk was likely established around 2.5 kyr BP, as the wave energy along the north coast precludes the existence of present-day fringing mangroves, and oceanographic conditions have probably remained stable since the mid-Holocene (Meltzner et al., 2017). Given the lack of ages on the sandy barrier, we do not know when it started to form, but the tidal creek that bends eastward while passing through it (Figure 5) suggests that the barrier has also been prograding eastward, consistent with the strong west monsoon on Belitung (Pamungkas, 2018).

Relative sea level fall between ~4 and ~2.5 kyr BP probably marked the onset of mangrove extension around Belitung. At all cross-sections, the reef that had formed in the few thousand preceding years could then provide a low-sloping substrate in the intertidal zone, which was no longer suitable for most coral species to grow given the occasional subaerial exposure but ideal for mangroves. Although we do not have the ages of the oldest mangrove sediments directly above the reef system deposits, we note that comparable mangrove deposits on Sungai Padang, Belitung (~25 km eastward from Sijuk), reported by Yulianto et al. (2019), recorded events of sea level regression dating back to at least 1.5 kyr BP. The chronology of mangrove development in Belitung closely resembles that of Krabi Province, Andaman Sea (Punwong et al., 2024). In Petaling and Sijuk, prograding mangroves have completely covered mid-Holocene reef flats, but in Batu Itam-Temparan, this process is still ongoing, as attested by pioneering *Rhizophora* mangroves that appear seawards of the mangrove forest on the fossil reef flat (Figure 9). Living reefs have migrated seawards since the relative sea level fall, and they are now mostly found as isolated patch reefs, both close to the shoreline and up to a few km seawards (Figures 1 and 5–7). We have illustrated the Holocene coastal landscape evolution of the Batu Itam-Temparan sections in Figure 9.

The three coastal sections analysed in this study provide some key similarities and differences. The most striking similarity between the three coastal sections is that the geological evolution of the early-mid Holocene reef system has been pivotal to the subsequent development of mangrove forests. It calls into question to what extent this finding constitutes a generic characteristic for Holocene tropical coastline evolution on the larger scale. With the exception of the N-Caribbean region, most of the world's tropical coastlines experienced a mid-Holocene highstand with a (slow) relative sea level fall since then (Khan et al., 2015). It would make sense that a lot of mangroves on those coastlines, in particular the 'open coast' (e.g., Worthington et al., 2020) or 'fringing' (e.g., Kathiresan, 2021) type mangroves like those in Petaling and Batu Itam-Temparan, benefitted from prior early to mid-Holocene reef formation, allowing for a vast expansion during relative sea level fall. Yet this geological preconditioning has so far been largely ignored in studies on Holocene mangrove evolution. In the case of deltaic and estuarine-type mangroves, the mid- to late-Holocene sea level fall seems to have had opposite effects, with decreased mangrove occupation in large river systems in Vietnam, Australia and Cambodia (Tanabe et al., 2003; Thom et al., 1975; Woodroffe et al., 1985; Woodroffe & Horton, 2005). At these locations the accretion and progradation of

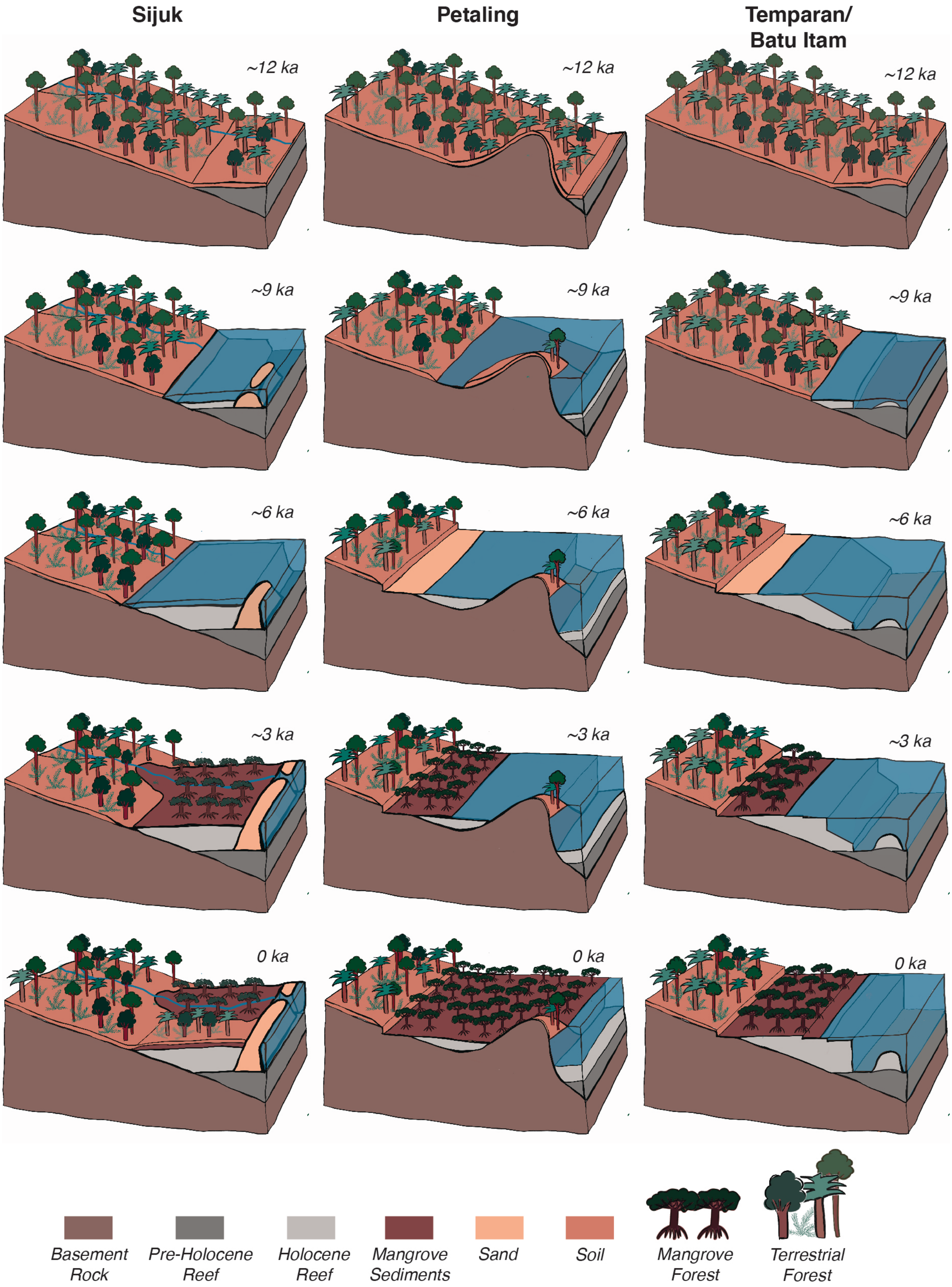

FIGURE 9 Coastal landscape evolution from early Holocene to current conditions showing chronology of Holocene coral reef and mangrove interplay for the Sijuk, Petaling and Batu Itam-Temparan sections. Note that the first two panels are not based on chronological constraints, other than descriptions of a quaternary reef unit at −20 to −30 m (Sarr et al., 2019), and are only speculative. At all locations, mangroves prograde over Holocene reefs following a change from sea level transgression (>6 ka) to regression (<6 ka). In Sijuk, the high wave energy led to the formation of sand barriers, providing a low-energy environment for the development of lagoonal/estuarine reefs and mangroves. In Petaling and Batu Itam-Temparan, a fringing reef/mangrove system developed instead, with pronounced effects of initial topography leading to mangroves either growing on top of fossil reefs or basement rocks. We suggest that isolated patch reefs in front of the Batu Itam-Temparan fringing reef (Figure 7) formed on irregularities of the pre-Holocene topography. Modified from Erkan and de Gelr (2025).

delta systems led to an increase in salt marshes, freshwater wetlands, and terrestrial forests at the expense of mangroves (Saintilan et al., 2020). Interestingly, this also seemed to have happened in Sijuk at a much smaller scale, as the mangrove sediments in the open-pit mine (S19-2; Figures 4 and 5) are overlain by peat deposits and modern terrestrial forest soil. The location of S19-2, where mangroves used to be present, is almost ∼1 km away from the current mangrove limit, suggesting that the mangrove extent has been strongly reduced as sediments filled in the former lagoon/estuary during relative sea level fall.

There is a main difference in wave energy between the three sites (see previous section), which dictated the coastal morphology: a sandy barrier with tidal creeks/estuarine mangroves for the highest wave energy environment (Sijuk; Figure 5) and fringing reefs with open-coast mangroves for the lower wave energy environments (Petaling and Batu Itam-Temparan; Figures 6 and 7). Furthermore, we propose that the lower wave energy in Petaling, compared to Batu Itam-Temparan, allowed the mangroves to fill up all the available accommodation space until the shoreline (1–2 km; Figure 6), whereas in Batu Itam-Temparan, only around 25% of the intertidal reef flat is occupied by mangroves (∼300–400 m; Figure 7). There may be a difference in sediment supply between Petaling and Batu Itam-Temparan, but we do not see clear reasons for that. Other differences between the sections include the presence of basement topographic and bathymetric features that are more pronounced in Sijuk and Petaling, although in all cases the basement topography puts a sharp landward limit on the spatial extent of the mangrove forests.

The future of Belitung's coral reefs and mangroves during 21st century relative sea level rise (RSLR) will depend on several factors, including reef growth conditions, sediment aggradation, temperature changes, wave erosion, monsoon changes and oceanographic conditions. For the open-coast mangroves on Belitung, there is little accommodation space landward, with the basement topography sharply increasing at the current mangrove limits (Figures 6 and 7). As such, both sediment aggradation and vertical reef growth will probably have to keep up with rates of RSLR if they are to maintain their surface area. A few examples indicate that coral reefs keep up with current sea level rise on reef flats (as in the Andaman Sea, Brown et al., 2011). If aggradation rates are lower, mangroves are at higher risk of drowning. If reef growth rates are lower, water depths will increase, which will likely increase wave erosion of the mangroves. RSLR rates for nearby Singapore are predicted to rise to ∼4, ∼8 and ∼12 mm/year by the year 2100 under representative concentration pathway (RCP) scenarios 1.9, 4.5 and 8.5, respectively (Shaw et al., 2023). Although the limited ages and aggradation rates obtained in our study are subject to high uncertainties (Figure 8) and might not be representative of the near future under different conditions than the mid-Holocene, none of them are as high as the rates associated with the middle and higher RCP scenarios. Predicting the future response of mangrove systems to RSLR is difficult and likely to be spatially heterogeneous and subjected to threshold responses, but our findings suggest a serious RSLR threat to the future of the Petaling and Batu Itam-Temparan mangroves. The case of Sijuk is different in the sense that the sandy barrier is several meters above PMSL and can shield the mangroves behind it from increased wave energy while taking advantage of the network of the protected tidal creeks behind it. Furthermore, most of the terrestrial forests that developed on top of the mangrove sediments around S19–2 have their ground level at ∼2- to 3-m elevation (Figure 5), which would potentially allow mangroves to partially re-accommodate those vast areas under the different RSLR scenarios.

Global compilations of Holocene mangrove sites suggest that most mangroves could only develop when RSLR fell below ∼7 mm/year (Saintilan et al., 2020, 2023) in the early to mid-Holocene. Modern-day sea level rise is currently estimated around 4 mm/year, and it is estimated to increase in the following decades (Cazenave & Llovel, 2010; IPCC, 2021; Mitchum et al., 2010; Rahmstorf, 2007). Although we imagine these RSLR rates will provide severe challenges to the survival of mangrove forests, we also emphasize that the starting point will be completely unique this time around. Just like the early- to mid-Holocene coral reef systems preconditioned to a suitable mangrove substrate, undoubtedly affecting RSLR thresholds for mangrove growth in that period, the current period of sea level rise is developing on top of a more complex Holocene coastal geomorphology that evolved over a longer period of time. As such, RSLR thresholds for mangrove survival will likely be very context-dependent in terms of mangrove type, like the open-coast and river-estuarine mangroves in this study, and also in terms of geological preconditioning. In line with the concept of biogeomorphological inheritance (Woodroffe, 2025), we propose that characterization and quantification of Holocene reef growth, mangrove formation, sedimentation and wave erosion in relation to coastal evolution may provide key insights to a tailored anticipation of future RSLR scenarios in mangrove preservation strategies.

7 | CONCLUSION

This case study from Belitung Island, Indonesia, offers a new insight into the interplay between coral reefs and mangroves in response to the Holocene sea level changes. We relate distinct sedimentary facies, including mangroves and deposits from the adjacent coral reef system, as well as the chronology of their development, itself tied to sea level changes. The Holocene sea level rise led to the establishment of nearshore reefs on Belitung Island from ∼6.5 to ∼4 kyr BP at an elevation between ∼1.8 m below PMSL and 0.8 m above PMSL. Following the formation of the nearshore reef and subsequent sea level fall, mangroves benefitted from the now-abandoned reef flat to develop and prograde seaward since at least the late Holocene (2.7–2.3 kyr BP) until the present day, with a thickness of more than 2.5 m in the sheltered Sijuk area and up to 2 m at the open-coast sites in Petaling.

Current findings contribute to our understanding of the geological and ecological processes that influence coastal ecosystems, providing insight into the complex interaction between coral reefs, mangroves and sea level changes throughout geological periods and the anticipated sea level rise on coastal ecosystems by the 21st century. Reef growth rates, sedimentation rates and wave energy all contribute to the historical and future development of the coastline, but sea level oscillations as modest as the mid-Holocene to late Holocene are even more critical for the determination of morphology on which coral reefs and mangroves develop. The extensive stretches of open-coast mangroves in the modern world could often owe their dimensions to the mid-Holocene development of coral reefs that converted during the late Holocene regression into large flats, conducive to the expansion of mangrove forests.

The fate of mangroves and coral reefs during the ongoing sea level rise depends not only on our ability to preserve the ecosystems but also on their geological preconditioning. Therefore, strategies to preserve mangrove ecosystems—while undoubtedly essential—can only be successful if accounting for their geological history.

ACKNOWLEDGEMENTS

We thank the 2 anonymous reviewers for their excellent suggestions and encouragements to improve this manuscript. DAU thanks RIIM LPDP and BRIN for the research grants in 2026 (batch 10) numbers B-847/II.7.5/FR.00.03/2/2026 and B-1158/III.4/FR00.03/2/2026. GdG acknowledges postdoctoral funding from the IRD and the Manajemen Talenta BRIN fellowship program, and research permit 52/SIP/IV/FR/6/2022 was provided by the Indonesian government on 8 June 2022. Radiocarbon dating has been carried out at the LMC14 laboratory (Saclay, France) with financial support from the IRD postdoctoral funding to GdG. RR acknowledges the Program PDKN Nusantara Research Grant number 083/E5/PG.02.00.PT/2022. Finally, it must be noted that this research would not have been possible without the indispensable support of local authorities, including Etyn Yunita (Belitong Geopark) and our local scientific field guides Stéphane and Yadi (Go Belitung). Open access publication funding provided by COUPERIN CY26.

CONFLICT OF INTEREST STATEMENT

The authors declare that they have no known competing financial interests or personal relationships that could have appeared to influence the work reported in this paper.

DATA AVAILABILITY STATEMENT

The data that support the findings of this study are available on request from the corresponding author. The data are not publicly available due to privacy or ethical restrictions.

PERMISSION TO REPRODUCE MATERIAL FROM OTHER SOURCES

I have nothing to declare.

ORCID

Tubagus Solihuddin https://orcid.org/0000-0002-1224-7487
Frida Sidik https://orcid.org/0000-0001-7329-9937
Laurent Husson https://orcid.org/0000-0002-9585-9074

REFERENCES

Allen Coral Atlas. (2022) Imagery, maps, and monitoring of the world's tropical coral reefs. https://doi.org/10.5281/zenodo.3833242

Alongi, D.M. (2008) Mangrove forests: resilience, protection from tsunamis, and responses to global climate change. *Estuarine, Coastal and Shelf Science*, 76(1), 1–13. Available from: https://doi.org/10.1016/j.ecss.2007.08.024

BIG. (2024) Bathymetry of Belitung Island, Bangka Belitung. https://tanahair.indonesia.go.id/demnas/#/batnas. Accessed 26 May 2024

Bird, M.I., Austin, W.E., Wurster, C.M., Fifield, L.K., Mojtahid, M. & Sargeant, C. (2010) Punctuated eustatic sea-level rise in the early mid-Holocene. *Geology*, 38(9), 803–806. Available from: https://doi.org/10.1130/G31066.1

Bird, M.I., Fifield, L.K., Teh, T.S., Chang, C.H., Shirlaw, N. & Lambeck, K. (2007) An inflection in the rate of early mid-Holocene eustatic sea-level rise: a new sea-level curve from Singapore. *Estuarine, Coastal and Shelf Science*, 71(3–4), 523–536. Available from: https://doi.org/10.1016/j.ecss.2006.07.004

Brown, B.E., Dunne, R.P., Phongsuwan, N. & Somerfield, P.J. (2011) Increased sea level promotes coral cover on shallow reef flats in the Andaman Sea, eastern Indian Ocean. *Coral Reefs*, 30(4), 867–878. Available from: https://doi.org/10.1007/s00338-011-0804-9

Buddemeier, R.W. & Smith, S.V. (1988) Coral reef growth in an era of rapidly rising sea level: predictions and suggestions for long-term research. *Coral Reefs*, 7(1), 51–56. Available from: https://doi.org/10.1007/BF00301982

Cabioch, G., Montaggioni, L.F., Faure, G. & Ribaud-Laurenti, A. (1999) Reef coralgal assemblages as recorders of paleobathymetry and sea level changes in the indo-Pacific province. *Quaternary Science Reviews*, 18(14), 1681–1695. Available from: https://doi.org/10.1016/S0277-3791(99)00014-1

Cahyarini, S.Y., Pfeiffer, M., Reuning, L., Liebetrau, V., Dullo, W.C., Takayanagi, H., et al. (2021) Modern and sub-fossil corals suggest reduced temperature variability in the eastern pole of the Indian Ocean dipole during the medieval climate anomaly. *Scientific Reports*, 11(1), 14952. Available from: https://doi.org/10.1038/s41598-021-94465-1

Cazenave, A. & Llovel, W. (2010) Contemporary Sea level rise. *Annual Review of Marine Science*, 2(1), 145–173. Available from: https://doi.org/10.1146/annurev-marine-120308-081105

Choudhary, B., Dhar, V. & Pawase, A.S. (2024) Blue carbon and the role of mangroves in carbon sequestration: its mechanisms, estimation, human impacts, and conservation strategies for economic incentives. *Journal of Sea Research*, 199, 102504. Available from: https://doi.org/10.1016/j.seares.2024.102504

Cobb, K.M., Westphal, N., Sayani, H.R., Watson, J.T., Di Lorenzo, E., Cheng, H., et al. (2013) Highly variable El Niño–southern oscillation throughout the Holocene. *Science*, 339(6115), 67–70. Available from: https://doi.org/10.1126/science.1228246

Collins, L.B., Testa, V., Zhao, J. & Qu, D. (2011) Holocene growth history and evolution of the Scott reef carbonate platform and coral reef. *Journal of the Royal Society of Western Australia*, 94(2), 239.

De Gelder, G., Husson, L., Pastier, A.M., Fernández-Blanco, D., Pico, T., Chauveau, D., et al. (2022) High interstadial sea levels over the past 420ka from the Huon peninsula, Papua New Guinea. *Communications Earth & Environment*, 3(1), 256. Available from: https://doi.org/10.1038/s43247-022-00583-7

De Gelder, G., Solihuddin, T., Utami, D.A., Hendrizan, M., Rachmayani, R., Chauveau, D., et al. (2023) Geodynamic control on Pleistocene coral reef development: insights from northwest Sumba Island (Indonesia). *Earth Surface Processes and Landforms*, 48(13), 2536–2553. Available from: https://doi.org/10.1002/esp.5643

Done, T.J. (1982) Patterns in the distribution of coral communities across the central great barrier reef. *Coral Reefs*, 1(2), 95–107. Available from: https://doi.org/10.1007/BF00301691

Dumoulin, J.P., Comby-Zerbino, C., Delque-Količ, E., Moreau, C., Caffy, I., Hain, S., et al. (2017) Status report on sample preparation protocols developed at the LMC14 laboratory, Saclay, France: from sample collection to 14C AMS measurement. *Radiocarbon*, 59(3), 713–726. Available from: https://doi.org/10.1017/rdc.2016.116

Embry, A.F. & Klovan, J.E. (1971) A late Devonian reef tract on northeastern Banks Island, NWT. *Bulletin of Canadian Petroleum Geology*, 19(4), 730–781.

Erkan, D. & de Gelr, G. (2025) Animation of coral reef mangrove evolution in Belitung figshare. Media. https://doi.org/10.6084/m9.figshare.29661044.v1

Falter, J.L., Lowe, R.J., Zhang, Z. & McCulloch, M. (2013) Physical and biological controls on the carbonate chemistry of coral reef waters: effects of metabolism, wave forcing, sea level, and geomorphology. *PLoS ONE*, 8(1), e53303. Available from: https://doi.org/10.1371/journal.pone.0053303

Fernández-Blanco, D., de Gelder, G., Lacassin, R. & Armijo, R. (2019) A new crustal fault formed the modern Corinth rift. *Earth-Science Reviews*, 199, 102919. Available from: https://doi.org/10.1016/j.earscirev.2019.102919ff

Geyh, M.A., Streif, H. & Kudrass, H.R. (1979) Sea-level changes during the late Pleistocene and Holocene in the strait of Malacca. *Nature*, 278(5703), 441–443. Available from: https://doi.org/10.1038/278441a0

Global Mangrove Watch. https://www.globalmangrovewatch.org/. accessed 15 August 2025.2025

Grossman, E.E. & Fletcher, I.I.I., III. (2004) Holocene reef development where wave energy reduces accommodaton space, Kailua Bay, windward Oahu, Hawaii, U.S.a. *Journal of Sedimentary Research*, 74(1), 49–63. Available from: https://doi.org/10.1306/070203740049

Guannel, G., Arkema, K., Ruggiero, P. & Verutes, G. (2016) The power of three: coral reefs, seagrasses, and mangroves protect coastal regions and increase their resilience. *PLoS ONE*, 11(7), e0158094. Available from: https://doi.org/10.1371/journal.pone.0158094

Harborne, A.R., Mumby, P.J., Micheli, F., Perry, C.T., Dahlgren, C.P., Holmes, K.E., et al. (2006) The functional value of Caribbean coral reef, seagrass, and mangrove habitats to ecosystem processes. *Advances in Marine Biology*, 50, 57–189. Available from: https://doi.org/10.1016/S0065-2881(05)50002-6

Hesp, P.A., Hung, C.C., Hilton, M., Ming, C.L. & Turner, I.M. (1998) A first tentative Holocene sea-level curve for Singapore. *Journal of Coastal Research*, 14, 308–314. Available from: https://www.jstor.org/stable/4298779

Hibbert, F.D., Rohling, E.J., Dutton, A., Williams, F.H., Chutcharavan, P.M., Zhao, C., et al. (2016) Coral indicators of past sea-level change: a global repository of U-series dated benchmarks. *Quaternary Science Reviews*, 145, 1–56. Available from: https://doi.org/10.1016/j.quascirev.2016.04.019

Hopley, D., Smithers, S.G. & Parnell, K.E. (2007) *The geomorphology of the great barrier reef. Development, diversity, and change*. Cambridge: Cambridge University Press, p. 546.

Howard, J., Sutton-Grier, A. & Herr, D. (2017) Clarifying the role of coastal and marine systems in climate mitigation. *Frontiers in Ecology and the Environment*, 1(1), 42–50. Available from: https://doi.org/10.1002/fee.1451

Husson, L., Riel, N., Aribowo, S., Authemayou, C., de Gelr, G., Kaus, B.J.P., et al. (2022) Slow geodynamics and fast morphotectonics in the far east Tethys. *Geochemistry, Geophysics, Geosystems*, 23(1), e2021GC010167. Available from: https://doi.org/10.1029/2021GC010167

IPCC. (2021) Summary For Policymakers. In: Masson-Delmotte, V., Zhai, P., Pirani, A., Connors, S.L., Péan, C., Berger, S., *et al*. (Eds.) *Climate change 2021: the physical science basis. Contribution of working group I to the sixth assessment report of the intergovernmental panel on climate change*. Cambridge, United Kingdom, and New York, NY, USA: Cambridge University Press, pp. 3–32 https://doi.org/10.1017/9781009157896.001

Kamaludin, H.B. (2001) *Holocene sea level changes in Kelang and Kuantan, Peninsular Malaysia*. Durham University Retrieved from. https://etheses.dur.ac.uk/3786/

Kamila, A., Bandyopadhyay, J. & Paul, A.K. (2020) An assessment of geomorphic evolution and some erosion-affected areas of Digha-Sankarpur coastal tract, West Bengal, India. *Journal of Coastal Conservation*, 24(5), 60. Available from: https://doi.org/10.1007/s11852-020-00778-0

Kantamaneni, K., Rice, L., Du, X., Allali, B. & Yenneti, K. (2022) Are current UK coastal defenses good enough for tomorrow? An assessment of vulnerability to coastal erosion. *Coastal Management*, 50(2), 142–159. Available from: https://doi.org/10.1080/08920753.2022.2022971

Kathiresan, K. (2021) Mangroves: types and importance. In: *Mangroves: ecology, biodiversity, and management*. Singapore: Springer Singapore, pp. 1–31 https://doi.org/10.1007/978-981-16-2494-0_1

Kench, P.S. & Brander, R.W. (2006) Wave processes on coral reef flats: implications for reef geomorphology using Australian case studies. *Journal of Coastal Research*, 22(1), 209–223. Available from: https://doi.org/10.2112/05a-0016.1

Khan, N.S., Ashe, E., Shaw, T.A., Vacchi, M., Walker, J., Peltier, W.R., et al. (2015) Holocene relative sea-level changes from near-, intermediate-, and far-field locations. *Current Climate Change Reports*, 1(4), 247–262. Available from: https://doi.org/10.1007/s40641-015-0029-z

Kleypas, J.A. (1996) Coral reef development under naturally turbid conditions: fringing reefs near broad sound, Australia. *Coral Reefs*, 15(3), 153–167. Available from: https://doi.org/10.1007/BF01145886

Li, J., Knapp, D.E., Schill, S.R., Roelfsema, C., Phinn, S., Silman, M., et al. (2019) Adaptive bathymetry estimation for shallow coastal waters using planet dove satellites. *Remote Sensing of Environment*, 232, 111302. Available from: https://doi.org/10.1016/j.rse.2019.111302

Li, T., Chua, S., Tan, F., Khan, N.S., Shaw, T.A., Majewski, J., et al. (2023) Glacial isostatic adjustment modelling of the mid-Holocene sea-level highstand of Singapore and Southeast Asia. *Quaternary Science Reviews*, 319, 108332. Available from: https://doi.org/10.1016/j.quascirev.2023.108332

Mann, T., Bender, M., Lorscheid, T., Stocchi, P., Vacchi, M., Switzer, A.D., et al. (2019) Holocene Sea levels in Southeast Asia, Maldives, India, and Sri Lanka: the SEAMIS database. *Quaternary Science Reviews*, 219, 112–125. Available from: https://doi.org/10.1016/j.quascirev.2019.07.007

Mazda, Y., Wolanski, E., King, B., Sase, A., Ohtsuka, D. & Magi, M. (1997) Drag force due to vegetation in mangrove swamps. *Mangroves and Salt Marshes*, 1(3), 193–199. Available from: https://doi.org/10.1023/A:1009949411068

McGregor, H.V., Wilcox, P., Fischer, M.J., Phipps, S.J., Gagan, M.K., Wittenberg, A. & Chivas, A.R. (2022) Millennial to seasonal scale views of El Niño-Southern Oscillation from central Pacific corals

Meltzner, A.J., Switzer, A.D., Horton, B.P., Ashe, E., Qiu, Q., Hill, D.F., et al. (2017) Half-metre sea-level fluctuations on centennial timescales from mid-Holocene corals of Southeast Asia. *Nature Communications*, 8(1), 14387. Available from: https://doi.org/10.1038/ncomms14387

Mitchum, G.T., Nerem, R.S., Merrifield, M.A. & Gehrels, W.R. (2010) Modern sea-level-change estimates. In: Church, J.A., Woodworth, P.L., Aarup, T. & Wilson, W.S. (Eds.) *Understanding sea-level rise and variability*. Chichester: Wiley-Blackwell, pp. 122–142 https://doi.org/10.1002/9781444323276.ch5

Montaggioni, L.F. (2005) History of indo-Pacific coral reef systems since the last glaciation: development patterns and controlling factors. *Earth-Science Reviews*, 71(1), 1–75. Available from: https://doi.org/10.1016/j.earscirev.2005.01.002

Montaggioni, L.F. & Faure, G. (1997) Response of reef coral communities to sea-level rise: a Holocene model from Mauritius (Western Indian Ocean). *Sedimentology*, 44(6), 1053–1070. Available from: https://doi.org/10.1111/j.1365-3091.1997.tb02178.x

Moreau, C., Caffy, I., Comby, C., Delqué-Količ, E., Dumoulin, J.P., Hain, S., et al. (2013) Research and development of the Artemis 14C AMS facility: status report. *Radiocarbon*, 55(2), 331–337. Available from: https://doi.org/10.1017/S0033822200057441

Nathan, Y., Chua, S., Chong, A., Chan, N., Morgan, K., Switzer, A.D., et al. (2025) Rapid mangrove sediment accretion in late-Holocene paleochannels of Singapore. *The Holocene*, 35(3), 259–270. Available from: https://doi.org/10.1177/09596836241297646

Neal, J. & Hawker, L. (2023) FABDEM V1-2. https://doi.org/10.5523/bris.s5hqmjcdj8yo2ibzi9b4ew3sn. Accessed 15 March 2024

Neumann, A.C. (1985) Reef response to sea level rise: keep-up, catch-up, or give up. Proc. Fifth Intern. Coral Reef Congr. Tahiti 3 105–110

Nienhuis, J.H., Ashton, A.D., Edmonds, D.A., Hoitink, A.J.F., Kettner, A.J., Rowland, J.C., et al. (2020) Global-scale human impact on delta morphology has led to net land area gain. *Nature*, 577, 514–518. Available from: https://doi.org/10.1038/s41586-019-1905-9

Pamungkas, A. (2018) Karakteristik parameter oseanografi (pasang-surut, arus, dan gelombang) di perairan utara dan selatan Pulau Bangka. *Buletin Oseanografi Marina*, 7(1), 51–58. Available from: https://doi.org/10.14710/buloma.v7i1.19042 (in Indonesia).

Punwong, P., Englong, A., Marchant, R., Jirapinyakul, A., Suttiwong, A., Chirawatkul, P., et al. (2024) A multi-proxy reconstruction of the late Holocene vegetation dynamics in Krabi mangroves, Thailand Andaman Sea. *Quaternary Science Advances*, 13, 100133. Available from: https://doi.org/10.1016/j.qsa.2023.100133

Pusat Studi Gempa Nasional (PuSGeN). (2025) *Peta sumber dan bahaya gempa Indonesia tahun 2024*. Jakarta: Kementerian Pekerjaan Umum dan Perumahan Rakyat Available at: https://ciptakarya.pu.go.id/admin/assets/upload/galeri/gempa/2026/02/10/887359_0.%

20Final_BUKU_PETA_SUMBER_DAN_BAHAYA_GEMPA_2024_Publish.pdf (Accessed: 26 February 2026). (in Indonesia).

Rahmstorf, S. (2007) A semi-empirical approach to projecting future sea level rise. *Science*, 315(5810), 368–370. Available from: https://doi.org/10.1126/science.1135456

Ramsey, C.B. (2009) Bayesian analysis of radiocarbon dates. *Radiocarbon*, 51(1), 337–360. Available from: https://doi.org/10.1017/s0033822200033865

Rogers, A. & Mumby, P.J. (2019) Mangroves reduce the vulnerability of coral reef fisheries to habitat degradation. *PLoS Biology*, 17(11), e3000510. Available from: https://doi.org/10.1371/journal.pbio.3000510

Saintilan, N., Horton, B., Törnqvist, T.E., Ashe, E.L., Khan, N.S., Schuerch, M., et al. (2023) Widespread retreat of coastal habitat is likely at warming levels above 1.5 C. *Nature*, 621(7977), 112–119. Available from: https://doi.org/10.1038/s41586-023-06448-z

Saintilan, N., Khan, N.S., Ashe, E., Kelleway, J.J., Rogers, K., Woodroffe, C.D., et al. (2020) Thresholds of mangrove survival under rapid sea level rise. *Science*, 368(6495), 1118–1121. Available from: https://doi.org/10.1126/science.aba2656

Sarr, A.C., Husson, L., Sepulchre, P., Pastier, A.-M., Pedoja, K., Elliot, M., et al. (2019) Subsiding Sundaland. *Geology*, 47(2), 119–122. Available from: https://doi.org/10.1130/G45629.1

Scheffers, A., Brill, D., Kelletat, D., Brückner, H., Scheffers, S. & Fox, K. (2012) Holocene Sea levels along the Andaman Sea coast of Thailand. *The Holocene*, 22(10), 1169–1180. Available from: https://doi.org/10.1177/0959683612441803

Scoffin, T.P. & Tissier, M.L. (1998) Late Holocene sea level and reef-flat progradation, Phuket, South Thailand. *Coral Reefs*, 17(3), 273–276. Available from: https://doi.org/10.1007/s003380050128

Shaw, T.A., Li, T., Ng, T., Cahill, N., Chua, S., Majewski, J.M., et al. (2023) Deglacial perspectives of future sea level for Singapore. *Communications Earth & Environment*, 4(1), 204. Available from: https://doi.org/10.1038/s43247-023-00868-5

Solihuddin, T., Bufarale, G., Blakeway, D. & O'Leary, M.J. (2016a) Geomorphology and late holocene accretion history of Adele reef: a northwest Australian mid-shelf platform reef. *Geo-Marine Letters*, 36(6), 465–477. Available from: https://doi.org/10.1007/s00367-016-0465-3

Solihuddin, T., Collins, L.B., Blakeway, D. & O'Leary, M.J. (2015) Holocene coral reef growth and sea level in a macrotidal, high turbidity setting: Cockatoo Island, Kimberley bioregion, Northwest Australia. *Marine Geology*, 359, 50–60. Available from: https://doi.org/10.1016/j.margeo.2014.11.011

Solihuddin, T., O'Leary, M.J., Blakeway, D., Parnum, I., Kordi, M. & Collins, L.B. (2016b) Holocene reef evolution in a macrotidal setting: Buccaneer Archipelago, Kimberley Bioregion, Northwest Australia. *Coral Reefs*, 35(3), 783–794. Available from: https://doi.org/10.1007/s00338-016-1424-1

Srivastava, J. & Prasad, V. (2019) Evolution and paleobiogeography of mangroves. *Marine Ecology*, 40(6), e12571. Available from: https://doi.org/10.1111/maec.12571

Sui, C., de Vos, P., Stapersma, D., Visser, K. & Ding, Y. (2020) Fuel consumption and emissions of ocean-going cargo ship with hybrid propulsion and different fuels over voyage. *Journal of Marine Science and Engineering*, 8(8), 588. Available from: https://doi.org/10.3390/jmse8080588

Susanto, R.D., Gordon, A.L. & Zheng, Q. (2001) Upwelling along the coasts of Java and Sumatra and its relation to ENSO. *Geophysical Research Letters*, 28(8), 1599–1602. Available from: https://doi.org/10.1029/2000GL011844

Susilohadi, S., Novico, F., Husson, L., Rahardiawan, R., Prabowo, H., Widodo, J., et al. (2024) Quaternary deposition and erosion in the northeastern Sunda Strait: an interplay between sea level, tectonics, and magmatic activity. *Journal of Asian Earth Sciences: X*, 12, 100179. Available from: https://doi.org/10.1016/j.jaesx.2024.100179

Suyarso, S. (2012) Melacak Perubahan Muka Laut Masa Lampau Berdasar Fosil Kerang-kerangan (Ostrea sp.) di Pulau Belitung. *Ilmu Kelautan: Indonesian Journal of Marine Sciences*, 15(3), 135–142. Available from: https://doi.org/10.14710/ik.ijms.15.3.135-142

Takahashi, T. (1988) Relationship between reef growth and sea level on the northwest coast of Kume Island, the Ryukyus: date from drill holes on the Holocene coral reef. Proceedings of the sixth international coral reef symposium, Townsville, Australia, 8th-12th August 1988, volume 3: contributed papers 491–496). The 6th International Coral Reef Symposium Executive Committee.

Tanabe, S., Hori, K., Saito, Y., Haruyama, S., Vu, V.P. & Kitamura, A. (2003) Song Hong (Red River) delta evolution related to millennium-scale Holocene Sea level changes. *Quaternary Science Reviews*, 3791(03), 2345–2361. Available from: https://doi.org/10.1016/S0277-3791(03)00138-0

Thom, B.G., Wright, L.D. & Coleman, J.M. (1975) Mangrove ecology and deltaic-estuarine geomorphology: Cambridge Gulf-Ord River, Western Australia. *The Journal of Ecology*, 63(1), 203–232. Available from: https://doi.org/10.2307/2258851

Tjia, H.D. (1996) Sea-level changes in the tectonically stable Malay-Thai peninsula. *Quaternary International*, 31, 95–101. Available from: https://doi.org/10.1016/1040-6182(95)00025-E

Tjia, H.D. & Liew, K.K. (1996) Changes in tectonic stress field in northern Sunda shelf basins. *Geological Society, London, Special Publications*, 106(1), 291–306. Available from: https://doi.org/10.1144/GSL.SP.1996.106.01.19

Tjia, H.D., Fujii, S. & Kigoshi, K., (1983). Holocene shorelines of Tioman island in the South China Sea. In: Terwindt, J., J. H, Van Steijn, H. (Eds.), Developments in physical geography - a tribute to J. I. S. Zonneveld, pp. 599e604.

van Woesik, R. & Done, T.J. (1997) Coral communities and reef growth in the southern great barrier reef. *Coral Reefs*, 16(2), 103–115. Available from: https://doi.org/10.1007/s003380050064

Veron, J.E.N. (2000) *Corals of the world*, Vol. 3. Townsville, Queensland, Australia: Australian Institute of Marine Science.

Wells, S. & Ravilious, C. (2006) In the front line: shoreline protection and other ecosystem services from mangroves and coral reefs (No. 24). UNEP/Earthprint.

Whitfield, A.K. (2017) The role of seagrass meadows, mangrove forests, salt marshes, and reed beds as nursery areas and food sources for fishes in estuaries. *Reviews in Fish Biology and Fisheries*, 27(1), 75–110. Available from: https://doi.org/10.1007/s11160-016-9454-x

Woodroffe, C. (1992) Mangrove sediments and geomorphology. *Tropical Mangrove Ecosystems*, 41, 7–41. Available from: https://doi.org/10.1029/CE041

Woodroffe, C.D. (2002) *Coasts: form, process, and evolution*. Cambridge, UK: Cambridge University Press.

Woodroffe, C.D. (2025) Biogeomorphological inheritance: the legacy of past landforms constrains future tropical coastal landscapes. *Earth Surface Processes and Landforms*, 50(2), e70013. Available from: https://doi.org/10.1002/esp.70013

Woodroffe, C.D., Rogers, K., McKee, K.L., Lovelock, C.E., Mendelssohn, I.A. & Saintilan, N. (2016) Mangrove sedimentation and response to relative sea-level rise. *Annual Review of Marine Science*, 8(1), 243–266. Available from: https://doi.org/10.1146/annurev-marine-122414-034025

Woodroffe, C.D., Thom, B.G. & Chappell, J. (1985) Development of widespread mangrove swamps in mid-Holocene times in northern Australia. *Nature*, 317(6039), 711–713. Available from: https://doi.org/10.1038/317711a0

Woodroffe, S.A. & Horton, B.P. (2005) Holocene sea-level changes in the indo-Pacific. *Journal of Asian Earth Sciences*, 25(1), 29–43. Available from: https://doi.org/10.1016/j.jseaes.2004.01.009

Worthington, T.A., Zu Ermgassen, P.S., Friess, D.A., Krauss, K.W., Lovelock, C.E., Thorley, J., et al. (2020) A global biophysical typology of mangroves and its relevance for ecosystem structure and deforestation. *Scientific Reports*, 10(1), 14652. Available from: https://doi.org/10.1038/s41598-020-71194-5

Wyrtki, K. (1961) *Physical oceanography of the Southeast Asian waters*, Vol. 2. La Jolla, California: Scripps Institution of Oceanography, University of California.

Xu, T.F., Wei, Z.X., Susanto, R.D., Li, S.J., Wang, Y.G., Wang, Y., et al. (2021) Observed water exchange between the South China Sea and Java Sea through Karimata Strait. *Journal of Geophysical Research:*

Oceans, 126(2), e2020JC016608. Available from: https://doi.org/10.1029/2020JC016608

Yamano, H., Hori, K., Yamauchi, M., Yamagawa, O. & Ohmura, A. (2001) Highest-latitude coral reef at Iki Island, Japan. *Coral Reefs*, 20(1), 9–12. Available from: https://doi.org/10.1007/s003380100137

Yamano, H., Inoue, T., Adachi, H., Tsukaya, K., Adachi, R. & Baba, S. (2019) Holocene sea-level change and evolution of a mixed coral reef and mangrove system at Iriomote Island, Southwest Japan. *Estuarine, Coastal and Shelf Science*, 220, 166–175. Available from: https://doi.org/10.1016/j.ecss.2019.03.001

Yulianto, E., Rahardjo, A.T., Noeradi, D., Siregar, D.A. & Hirakawa, K. (2005) A Holocene pollen record of vegetation and coastal environmental changes in the coastal swamp forest at Batulicin, South Kalimantan, Indonesia. *Journal of Asian Earth Sciences*, 25(1), 1–8. Available from: https://doi.org/10.1016/j.jseaes.2004.01.005

Yulianto, E., Sukapti, W.S. & Praptisih, P. (2019) Perubahan Lingkungan dan Evolusi Mangrove di Pulau Belitung Selama Holosen Akhir Berdasarkan Rekaman Polen. *Jurnal Geologi Kelautan*, 17(2), 456124, Available from: https://doi.org/10.32693/jgk.17.2.2019.578 (in Indonesia).

How to cite this article: Solihuddin, T., de Gelder, G., Utami, D.A., Sidik, F., Rachmayani, R., Hendrizan, M. et al. (2026) Coral reef and mangrove interplay during Holocene sea level changes, Belitung Island, Indonesia. *Earth Surface Processes and Landforms*, 51(7), e70354. Available from: https://doi.org/10.1002/esp.70354